Zootaxa 4638 (2): 151–198
https://www.mapress.com/j/zt/

Article

ISSN 1175-5326 (print edition)
ZOOTAXA
ISSN 1175-5334 (online edition)

https://doi.org/10.11646/zootaxa.4638.2.1
http://zoobank.org/urn:lsid:zoobank.org:pub:FF159163-7F48-4FB3-B4DF-57527860EA36

Geographic structure of genetic variation in the Parachute Gecko *Ptychozoon lionotum* Annandale, 1905 across Indochina and Sundaland with descriptions of three new species

L. LEE GRISMER[1], PERRY L. WOOD JR.[2], JESSE L. GRISMER[1], EVAN S. H. QUAH[3], NEANG THY[4], SOMPHOUTHONE PHIMMACHAK[5], NIANE SIVONGXAY[5], SENGVILAY SEATEUN[5], BRYAN L. STUART[6], CAMERON B. SILER[7], DANIEL G. MULCAHY[8], TASHITSO ANAMZA[9] & RAFE M. BROWN[9]

[1]Herpetology Laboratory, Department of Biology, La Sierra University, 4500 Riverwalk Parkway, Riverside, California 92515, USA. E-mail: lgrismer@lasierra.edu. jgrismer@lasierra.edu
[2]Department of Biological Sciences & Museum of Natural History, Auburn University, Auburn, Alabama 36849, USA. E-mail: plw0013@auburn.edu
[3]School of Biological Sciences, Universiti Sains Malaysia, 11800 Minden, Penang, Malaysia. E-mail: evanquah@yahoo.com
[4]Wild Earth Allies, #77a, St. Betong, Bayab Village, Sk. Phnom Penh Thmei, Kh. Sen Sok, Phnom Penh, Cambodia. E-mail: thyneang9@gmail.com
[5]National University of Laos, Faculty of Natural Sciences, Department of Biology, P.O. Box 2273, Dong Dok Campus, Vientiane, Laos. E-mail: somphouthone26@hotmail.com, sivongxain@gmail.com, xang_s@yahoo.com
[6]Section of Research & Collections, North Carolina Museum of Natural Sciences, Raleigh, NC, USA. E-mail: bryan.stuart@naturalsciences.org
[7]Sam Noble Oklahoma Museum of Natural History and Department of Biology, University of Oklahoma, Norman, Oklahoma, 73072-7029, USA. E-mail: camsiler@ou.edu
[8]Global Genome Initiative, National Museum of Natural History, Smithsonian Institution, Washington, DC, 20013, USA. E-mail: MulcahyD@si.edu
[9]Department of Ecology and Evolutionary Biology and Biodiversity Institute, University of Kansas, Dyche Hall, 1345 Jayhawk Blvd, Lawrence, Kansas 66045-7561, USA. E-mail: rafe@ku.edu

Abstract

An integrative taxonomic analysis of the *Ptychozoon lionotum* group across its range in Indochina and Sundaland recovers *P. lionotum sensu lato* Annandale, 1905 as paraphyletic with respect to *P. popaense* Grismer, Wood, Thura, Grismer, Brown, & Stuart, 2018a and composed of four allopatric, genetically divergent, ND2 mitochondrial lineages. Multivariate and univariate analyses of continuous and discrete morphological and color pattern characters statistically and discretely diagnose each lineage from one another and together, with maximum likelihood and Bayesian inference analyses, provide the foundation for the recognition of each lineage as a new species—hypotheses corroborated with a Generalized Mixed Yule Coalescent species delimitation analysis. *Ptychozoon cicakterbang* **sp. nov.** ranges throughout Peninsular Malaysia to Pulau Natuna Besar, Indonesia; *P. kabkaebin* **sp. nov.** is endemic to northern and central Laos; and *P. tokehos* **sp. nov.** ranges from southern Thailand south of the Isthmus of Kra northward to Chiang Mai, fringing the Chao Phraya Basin and ranging southward through Cambodia to southern Vietnam. *Ptychozoon lionotum sensu stricto* ranges from northwestern Laos through southern Myanmar to eastern India. The phylogeographic structure within each species varies considerably with *P. lionotum s.s.* showing no genetic divergence across its 1,100 km range compared to *P. cicakterbang* **sp. nov.** showing upwards of 8.2% sequence divergence between syntopic individuals. Significant phylogeographic structure exists within *P. tokehos* **sp. nov.** and increased sampling throughout Thailand may require additional taxonomic changes within this species.

Key words: Asia, Gekkonidae, gliding, integrative taxonomy, phylogeography, species complex

Introduction

Parachute Geckos of the genus *Ptychozoon* Kuhl & van Hasselt, 1822 are among some of Asia's most intriguing lizards in that their highly specialized, nocturnal, arboreal lifestyle revolves around crypsis and parachuting

Accepted by A. Bauer: 12 May 2019; published: 16 Jul. 2019

or gliding from one tree to another. Despite a myriad of behavioral and morphological adaptations (Brown *et al.* 1997; Dudley *et al.* 2007; Heyer & Pongsapipatana 1970; Marcellini & Keefer 1976; Russell *et al.* 2001; Young *et al.* 2002) necessary to support this peculiar life style, the 10 nominal species manifest a considerable degree of morphological and color pattern variation among them that has enabled systematists to construct reasonably robust taxonomies for nearly two centuries (Gray 1827; Boulenger 1899; Stejneger 1902; Annandale 1905; Taylor 1915; Brown *et al.* 1997; Brown 1999; Das & Vijayakumar 2009; Sumontha *et al.* 2012; Wang *et al.* 2016; Grismer *et al.* 2018a). However, recent molecular-based phylogenetic reconstructions have revealed that the most widely distributed species, *P. kuhli* (Stejneger, 1902) and *P. lionotum* Annandale, 1905*,* are likely to be species complexes composed of deeply divergent, allopatric, mitochondrial lineages (Brown *et al.,* 2012; Grismer *et al.,* 2018a). In the most recent phylogeny delimiting the newest species of the genus *P. popaense*, Grismer *et al.* (2018a) noted—with limited sampling (N=8 mtDNA sequences and preserved specimens)—additional phylogeographic structure within *P. lionotum* across Myanmar, Thailand, Cambodia, and Laos in spite of the fact that their sampling did not include specimens from the southern extreme of this species' distribution in Peninsular Malaysia (Grismer 2011a). We extend that study here with increased sampling (N=36 mtDNA sequences and 44 preserved specimens) from across *P. lionotum*'s broad range including Peninsular Malaysia (Fig. 1). Our integrative taxonomic analysis not only recovered additional, highly divergent lineages bearing notable phylogeographic substructure, it also demonstrated that *P. lionotum* as currently constituted, is paraphyletic with respect to *P. popaense.* Therefore, in order to construct a taxonomy consistent with this groups' evolutionary history, we describe three new allopatric, phenotypically distinct, diagnosable, and divergent mitochondrial clades from Peninsular Malaysia, Thailand and Cambodia, and Laos, respectively. While conducting this study, we came across two specimens accessioned in their institutional collections as *P. lionotum* that represent significant range extensions of *P. kaengkrachanense* Sumontha, *et al.,* 2012 in Thailand as well as a new country record of *P. trinotaterra* Brown, 1999 for Laos. The descriptions and range extensions are discussed below.

Materials and methods

Species delimitation. The general lineage concept (GLC: de Queiroz 2007) adopted herein proposes that a species constitutes a population of organisms evolving independently from other such populations owing to a lack of gene flow. By "independently," it is meant that new mutations arising in one species cannot spread readily into another species (Barraclough *et al.* 2003; de Queiroz 2007). Integrative studies on the nature and origins of species are using an increasingly wider range of empirical data to delimit species boundaries (Coyne & Orr 1998; Fontaneto *et al.* 2007; Knowles & Carstens 2007, Leaché *et al.* 2009), rather than relying solely on morphology and traditional taxonomic methods. Under the GLC implemented herein, molecular phylogenies were used to recover monophyletic mitochondrial lineages of individuals from the same geographic areas (populations) in order to develop initial species-level hypotheses. Various univariate and multivariate analyses of morphological and color pattern data were then used to search for statistical concordance among those mitochondrial lineages in support of their hypothetical species-level designation (*i.e.,* species boundaries). These species boundaries were subsequently cross-checked using a Generalized Mixed Yule Coalescent (GMYC) approach (Pons *et al.* 2006), thus providing an additional framework to complement the empirically based hypotheses of the morphological and molecular analyses.

Molecular data and analyses. The final, aligned sequence dataset contained 47 ingroup samples representing eight of the 10 nominal species of *Ptychozoon*. Unfortunately, the sampling of tissue material from *P. nicobarense* Das & Vijayakumar, 2009 and *P. kaengkrachanense* Sumontha *et al.,* 2012 was neglected at the time of their collection. However, all species of the *P. lionotum* group (*sec.* Grismer *et al.* 2018a; *P. bannaense* Wang *et al.,* 2016, *P. popaense* Grismer *et al.,* 2018a, and *P. lionotum* Annandale, 1905) were represented in the ingroup sampling. *Pseudogeckko compressicorpus* (Taylor, 1915); *Pseudogekko smaragdinus* (Taylor, 1922); *Luperosaurus cumingii* (Gray, 1845); *L. angliit* Brown, Diesmos & Oliveros, 2011; *L. iskandari* Brown, Supriatna & Ota, 2000; *L. macgregori* Stejneger, 1907; *Ptychozoon rhacophorus* (Boulenger, 1899); and *Gekko vittatus* Houttuyn, 1782 composed the outgroups following Brown *et al.* (2012) in part and were used to root the tree. All new sequences were deposited in GenBank (Table 1).

TABLE 1. GenBank accession numbers for the ND2 sequence data for the specimens of *Ptychozoon* used for the molecular phylogenetic analyses. Numbers in parentheses refer to numbered localities in Figure 1.

Taxon	Catalog number	Locality	GenBank no.
Pseudogekko compressicorpus	KU 324426	Philippines, Bohol Province, Municipality of Sierra Bullones	JQ437898
Pseudogekko smaragdinus	KU 302819	Philippines, Quezon Province, Municipality of Polillo	JQ437897
Luperosaurus cumingii	TNHC 61910	Philippines, Luzon Island, Albay Province	JQ437902
Luperosaurus angliit	KU 322189	Philippines, Aurora Province, Municipality of Baler	JQ437903
Luperosaurus macgregori	KU 314021	Philippines, Batanes Province, Municipality of Basco	JQ437905
Ptychozoon rhacophorus	P 0500	East Malaysia, Sarawak, Gunung Penrissen	JQ437913
Gekko vittatus	USNM 533255	Solomon Islands, Santa Cruz Island, Temotu, Luesalo	JN019073
Luperosaurus iskandari	MZB 2114	Indonesia, Sulawesi Island, Central Sulawesi Province, ~ 4k E Dunsun Satu, Kecamatan, Pagimana, Kabupaten Banggai	JQ437906
Ptychozoon bannaense	SYS r001237	China, Yunnan, Mengyang, Xishuangbanna	KU570000
Ptychozoon bannaense	SYS r001242	China, Yunnan, Mengyang, Xishuangbanna	KU570001
Ptychozoon cicakterbang **sp. nov.**	JAM 1426 (4)	Ulu Gombak, Selangor, Peninsular Malaysia	JQ437916
Ptychozoon cicakterbang **sp. nov.**	LSUHC 5539 (2)	Pulau Sibu, Johor, Peninsular Malaysia	MK803392
Ptychozoon cicakterbang **sp. nov.**	LSUHC 5597 (2)	Pulau Sibu, Johor, Peninsular Malaysia	MK803391
Ptychozoon cicakterbang **sp. nov.**	LSUHC 5783 (9)	Temengor, Perak, Peninsular Malaysia	MK803390
Ptychozoon cicakterbang **sp. nov.**	LSUHC 6437 (3)	Tekek-Juara Trail, Pulau Tioman, Pahang, Peninsular Malaysia	JQ437917
Ptychozoon cicakterbang **sp. nov.**	LSUHC 8709 (8)	Pulau Perhentian Besar, Terengganu, Peninsular Malaysia	MK803386
Ptychozoon cicakterbang **sp. nov.**	LSUHC 9059 (8)	Pulau Perhentian Besar, Terengganu, Peninsular Malaysia	MK803385
Ptychozoon cicakterbang **sp. nov.**	LSUHC 9409 (7)	Reng Reef, Pulau Redang, Terengganu, Peninsular Malaysia	MK803381
Ptychozoon cicakterbang **sp. nov.**	LSUHC 9447 (13)	Gunung Machinchang, Pulau Langkawi, Kedah, Peninsular Malaysia	MK803389
Ptychozoon cicakterbang **sp. nov.**	LSUHC 9891 (10)	Lata Tembaka, Terengganu, Peninsular Malaysia	MK803387
Ptychozoon cicakterbang **sp. nov.**	LSUHC 10648 (12) holotype	Along the road to the top of Gunung Jerai, Kedah, Peninsular Malaysia	MK803388
Ptychozoon cicakterbang **sp. nov.**	LSUHC 10978 (5)	Hutan Lipur Lata Belatan, Terengganu, Peninsular Malaysia	MK803383
Ptychozoon cicakterbang **sp. nov.**	LSUHC 11234 (5)	Hutan Lipur Lata Belatan, Terengganu, Peninsular Malaysia	MK803379
Ptychozoon cicakterbang **sp. nov.**	LSUHC 11235 (10a)	Gunung Tebu, Terengganu, Peninsular Malaysia	MK803378
Ptychozoon cicakterbang **sp. nov.**	LSUHC 11236 (5)	Hutan Lipur Lata Belatan, Terengganu, Peninsular Malaysia	MK803384
Ptychozoon cicakterbang **sp. nov.**	LSUHC 11418 (6)	Pulau Bidong, Terengganu, Peninsular Malaysia	MK803382
Ptychozoon cicakterbang **sp. nov.**	LSUHC 11419 (6)	Pulau Bidong, Terengganu, Peninsular Malaysia	MK803380
Ptychozoon cicakterbang **sp. nov.**	LSUHC 11439 (6)	Pulau Bidong, Terengganu, Peninsular Malaysia	MK803377

.....continued on the next page

TABLE 1. (Continued)

Taxon	Catalog number	Locality	GenBank no.
Ptychozoon cicakterbang **sp. nov.**	LSUHC 11894 (2)	Pulau Sibu, Johor, Peninsular Malaysia	MK803376
Ptychozoon horsfieldii	ZRC 2.5339	East Malaysia, Sarawak, Lambir Hills	JQ437907
Ptychozoon intermedium	CMNH 4746	Philippines, Mindanao Island, Davo City Province, Municipality of Calinan Barangay Malagos, Baguio District.	JQ437908
Ptychozoon intermedium	CMNH 4747	Philippines, Mindanao Island, Davo City Province, Municipality of Calinan Barangay Malagos, Baguio District.	JQ437909
Ptychozoon intermedium	CMNH 4748	Philippines, Mindanao Island, Davo City Province, Municipality of Calinan Barangay Malagos, Baguio District.	JQ437910
Ptychozoon intermedium	TNHC 56144	Philippines, Mindanao Island, Davo City Province, Municipality of Calinan Barangay Malagos, Baguio District.	JQ437911
Ptychozoon kabkaebin **sp. nov.**	NUOL 00036 (32)	Laos, Khammouan Province, Boualapha District, Phou Ack	MH809360
Ptychozoon kabkaebin **sp. nov.**	NCSM 80585 (33) holotype	Laos, Bolikhamxay, Pakkading, Houay Ta Ang Stream	MH809359
Ptychozoon kuhli	LSUHC 4819	West Malaysia, Selangor, Kepong, FRIM	JX440536
Ptychozoon kuhli	LSUHC 7640	West Malaysia, Johor, Endau-Rompin	JQ437926
Ptychozoon kuhli	MVZ 239350	Indonesia, Sumatra, Kabupaten Bengkulu, Kecematan Kepahiang	JQ437922
Ptychozoon kuhli	MVZ 239588	Indonesia, Sumatra, Kabupaten Bengkulu, Kecematan Kepahiang	JQ437922
Ptychozoon kuhli	ND 7517	West Malaysia	JQ437928
Ptychozoon kuhli	RMB 1134	West Malaysia	JX041423
Ptychozoon lionotum	CAS 221168 (37)	Myanmar, Bago Division, Yemwe Reserve Forest, Chaung Gwa Village	JX041424
Ptychozoon lionotum	CAS 238865 (39)	Myanmar, Rakhine State, Kyaukpyu Dist, Yanbye Township, Chin Minbyin Village	MH809362
Ptychozoon lionotum	NCSM 79473 (36)	Laos, Luang Phabang, Province Tad Kuang Si Provincial Protected Area	MH809363
Ptychozoon lionotum	NCSM 79474 (36)	Laos, Luang Phabang, Province Tad Kuang Si Provincial Protected Area	MH809361
Ptychozoon tokehos **sp. nov.**	CUMZ.2005.07.30.40 (17)	Thailand, Nakkon Si Thammarat, Khao Luang National Park	JQ437914
Ptychozoon tokehos **sp. nov.**	FMNH 261853 holotype (25)	Cambodia, Kampong Speu Province, Phnom Srouch District	JQ437915
Ptychozoon tokehos **sp. nov.**	USNM 587523 (19)	Myanmar, Tanintharyi	MK803372
Ptychozoon tokehos **sp. nov.**	CBC 03162 (27)	Cambodia, Phnom Samkos	MK803374
Ptychozoon tokehos **sp. nov.**	NCSM 98986 (27)	Cambodia, Bokor National Park	MK803375
Ptychozoon tokehos **sp. nov.**	NCSM 98987 (27)	Cambodia, Bokor National Park	MK803373
Ptychozoon popaense	LSUHC 13507	Myanmar, Mandalay Division, Mt. Popa, Kyauk-pa-taung Township	MH809358
Ptychozoon popaense	LSUHC 13508	Myanmar, Mandalay Division, Mt. Popa, Kyauk-pa-taung Township	MH809357
Ptychozoon trinotaterra	ROM 31912	Vietnam, Dac Lac province, Yok Don, Yok Don National Park	JQ437912
Ptychozoon trinotaterra	NCSM 77915	Laos, Khammouan Province, Nakai District, WMPA headquarters, Nakai-Nam Theun National Protected Area	MK803371

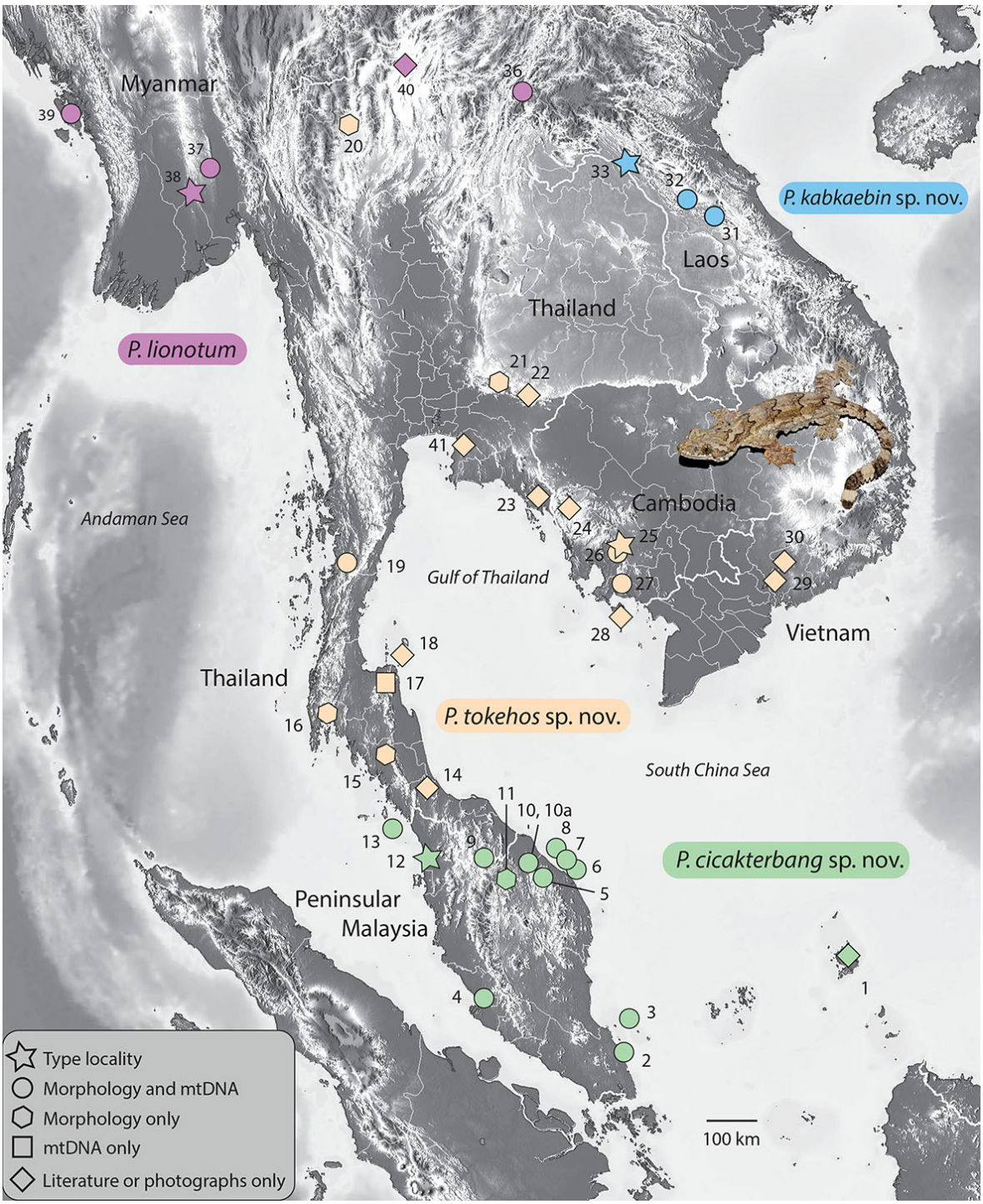

FIGURE 1. Distribution of *Ptychozoon lionotum*, *P. cicakterbang* **sp. nov.**, *P. kabkaebin* **sp. nov.**, and *P. tokehos* **sp. nov.** Diamond designated localities are non-specimen based and considered tentative. Their sources are: (1) Pulau Natuna Besar, Indonesia (Leong *et al*. 2003); (14) Hat Yai, Songkla, Thailand (LSUDPC 10946); (18) Ko Samui, Surat Thani, Thailand (LSUDPC 10948); (22) Dong Paya Fei Mounatains, Nakhon Ratchasima, Thailand (Smith 1935); (23) Chantabun, Chanthaburi, Thailand (Smith 1935); (24) Phnom Samkos, Pursat, Cambodia (LSUDPC 10949–53); (28) Phu Quoc Island, Kiem Giang Province, Vietnam (Nguyen *et al*. 2009); (29) Trang Bom, Dong Nai Province, Vietnam (Nguyen *et al*. 2009) however this specimen may be *P. trinotaterra* (see Distribution section for *P. tokehos* **sp. nov.**); (30) Cat Tien, Dong Nai Province, Vietnam (Nguyen *et al*. 2009); and (41) Siracha, Chanthaburi, Thailand (Smith 1935). Numbered locations for the specimen-based localities are listed in Tables 1 and 6–9 and on the tree in Figure 2.

Genomic DNA was isolated from liver or skeletal muscle (preserved in 95% ethanol or DMSO/EDTA solution) using the Maxwell® RSC Tissue DNA kit on the Promega Maxwell® RSC extraction robot or on an AutoGenprep 965 (AutoGen, Inc.) with an overnight digestion in proteinase-K and M1–2 buffers and the standard animal protocols. We amplified a fragment of ND2 using a double-stranded Polymerase Chain Reaction (PCR) under Grismer *et al*.'s (2018a) conditions: 1.0 µl DNA, 1.0 µl light strand primer 1.0 µl heavy strand primer, 1.0 µl dinucleotides, 2.0 µl 5x buffer, MgCl 10x buffer, 0.1 µl Taq polymerase, and 7.56 µl ultra-pure H2O (Grismer *et al*. 2018a). We performed PCR reactions on Bio-Rad gradient thermocyclers under the following conditions: (1) denaturation, 95°C, 120 s, (2) second denaturation, 95°C, 35 s, (3) annealing, 48–50°C, 35 s, (4) extension, 72°C, 35 s (5) repeated steps 2–4 for 31 cycles. Successful PCR products (visualized on agarose gels) were outsourced to GENEWIZ® for PCR purification, cycle and sequencing, or were purified using ExoSap-IT™ and sequenced in both directions using a BigDye® Terminator v3.1 Cycle Sequencing kit on an Automated ABI3730 Sequencer (Life Technologies). All were sequenced using the same primers as in the amplification step (Table 2). Sequences were determined in both directions to confirm congruence and both reads were edited in GeneiousTM version v6.1.8 (Drummond *et al.* 2011). The ND2 protein-coding region and the three tRNAs were aligned using the MAFTT v7.017 (Katoh & Kuma 2002) plugin under default settings available in GeneiousTM. We calculated the correct amino acid reading frame for the protein coding region and confirmed the absence of stop codons in Mesquite v3.04 (Maddison & Maddison 2015).

TABLE 2. Primer sequences used in this study for amplification and sequencing the ND2 gene and the flanking tRNAs.

Primer name	Primer reference		Sequence
L4437b	(Macey *et al.* 1997)	External	5'-AAGCAGTTGGGCCCATACC-3'
H5934	(Macey *et al*. 1997)	External	5' -AGRGTGCCAATGTCTTTGTGRTT-3'

Two model-based phylogenetic analyses, maximum likelihood (ML) and Bayesian Inference (BI), were employed to reconstruct the evolutionary history of *Ptychozoon*. The ML analysis was implemented in IQ-TREE (Nguyen *et al.* 2015) and used a Bayesian Information Criterion (BIC) to calculate that HKY+F+G4 was the best-fit model of evolution for the tRNA, GTR+F+I+G4 the best-fit model for the first codon position, TIM3+F+I+G4 for the second codon position, and TIM2+F+I+G4 for the third codon position. Ultrafast Bootstrap Approximation (UFB; Hoang *et al.* 2017) using 1000 bootstrap replicates was used to construct a final consensus tree. Nodes with UFB values of 95 and above were considered significantly supported. A BI analysis was implemented in MrBayes 3.2.3. on XSEDE (Ronquist *et al.* 2012) using CIPRES (Cyberinfrastructure for Phylogenetic Research; Miller *et al.* 2010) employing default priors and a GTR+I+Gamma model of evolution for all codon positions. Two simultaneous runs were performed with four chains, three hot and one cold. The simulation ran for 10,000,000 generations, was sampled every 1000 generations using the Markov Chain Monte Carlo (MCMC), and the first 25% of each run were discarded as burn-in. Stationarity from each run was checked in Tracer v1.6 (Rambaut *et al.* 2014) to ensure effective sample sizes (ESS) were above 200 for all parameters. Nodes with Bayesian posterior probabilities (BI) of 0.95 and above were considered well-supported (Huelsenbeck *et al.* 2001; Wilcox *et al.* 2002). After removing all species except those in the *P. lionotum* group, MEGA7 (Kumar *et al.* 2016) was used to calculate uncorrected pairwise sequence divergences among the individuals.

An ultrametric tree generated in BEAST v2.4.6 (Bayesian Evolutionary Analysis Sampling Trees; Drummond *et al.* 2012) was used to perform the Generalized Mixed Yule Coalescent (GMYC) approach to species delimitation (Pons *et al.* 2006), thus providing an additional framework to complement the empirically based thresholds of the BI and ML analyses. The BEAST analysis was implemented in BEAUti version v2.4.7 (Bayesian Evolutionary Analysis Utility) and run with BEAST v2.4.6 on CIPRES employing a lognormal relaxed clock with unlinked substitution and clock models and an HKY substitution model selected for each codon position. MCMC chains were run using a coalescent exponential population prior for 100,000,000 million generations and logged every 10,000 generations. The BEAST log file was visualized and checked in Tracer v1.6.0 (Rambaut *et al.* 2014) to ensure ESS values were above 200 for all parameters. A maximum clade credibility tree using mean heights at the nodes was generated using TreeAnnotator v.1.8.0 (Rambaut & Drummond 2013) with a burnin of 1000 trees (10%).

The GMYC approach is a method for delimiting species from single-locus, time-calibrated ultrametric gene trees by detecting genetic clustering beyond the expected levels of a null hypothesis which infers that all individuals of a population form a genetically, interacting nexus. In clades where effective population sizes are not necessarily

low and divergence times among the populations are not high, the multi-threshold version of the model (such as that used herein) out performs the single-threshold version (Fujisawa & Barraclough 2013). The GMYC relies on the prediction that independent evolution leads to the appearance of distinct genetic clusters, separated by relatively longer internal branches (Barraclough *et al.* 2003; Acinas *et al.* 2004). Such groups therefore, diverge into discrete units of morphological and genetic variation that are recovered with surveys of higher clades. The analysis was run on a web server at http://species.h-its.org/gmyc/ on 26 December 2018.

Morphological data and analyses. Mensural data were taken on the right side of the body when possible to the nearest 0.1 mm using dial calipers under a Leica Wild M 10 stereo dissecting microscope following character definitions modified from Brown *et al.* (1997), Brown (1999), and Grismer *et al.* (2018a). Characters examined were SVL = snout-vent length, from the tip of snout to the vent; HD = head depth, the maximum thickness of the head posterior to the eyes; HL = head length, from the posterior margin of the retroarticular process to the tip of the snout; HW = head width, across the angle of the jaws; ED = eyeball diameter, the greatest horizontal diameter of the eyeball; SNL = snout length, from the anterior margin of the orbit on the prefrontal bone to the tip of the snout; TD = tympanum diameter, the greatest horizontal distance across the auricular opening; IN = internarial distance, measured between the nares across the rostrum; IO = interorbital distance, from between the anterior edges of the prefrontal bones anterior to the eyeballs; AXG = axilla-groin length, from the posterior margin of the forelimb insertion to the anterior margin of the hind limb insertion; FL = forearm length, from the posterior margin of the elbow while flexed 90° to the dorsal inflection of the wrist while flexed 90°; TBL = tibia length, from the posterior surface of the knee while flexed 90° to the dorsal inflection of the ankle while flexed 90°; TL = tail length, from the vent to the tip of the tail; and TW = tail width, distance across the body of the tail (caudal lobes not included) at the insertion point of the postfemoral flaps.

Meristic characters following Brown *et al.* (1997), Brown (1999), and Grismer *et al.* (2018a) and included the number of supralabials (SU) counted from the rostral scale to below the middle of the eyeball. Scales posterior to this point transition smoothly into the granular scales at the commissure of the jaw and determining where the enlarged supralabials stop and the granular scales start is too subjective. Therefore, supralabials posterior to the middle of the eyeball were not counted. Infralabials (IL) counted from the mental scale to their termination at the commissure of the jaw (they do not imperceptively transition into granular scales); midbody dorsal scales (MB), the granular scales counted midway between the limb insertions transversely across the body from the base of one patagium to the other; enlarged ventral scales (VS) counted across the belly from the medial termination points of the granular scales on the lower portion of the flanks where they transition into the larger, flat ventral scales; number of enlarged pore-bearing precloacal scales (PP) in males; enlarged precloacal scales (PS) in both sexes counted as the enlarged, flat scales that begin in the proximal region of the thighs and extend uninterrupted across the precloacal region; number of enlarged post-precloacal scales (PPS) counted from the middle of the enlarged precloacal scale row to the edge of the granular scales anterior to the vent; transversely expanded subdigital lamellae on fingers and toes I–V were counted only as those scales that extend completely across the width of the digit regardless if there are enlarged scales proximal to these or not. Enlarged subdigital scales extend onto the palmar and plantar surfaces and transition into the scales of those surfaces, making it too subjective to determine where the counting should begin or end. As such, these counts have varied widely among different authors. Scale counts from digits IV on the foot (TL4) were used in the statistical analyses. The estimated number of scales across the widest portion of terminal caudal flap (CF). This count was imprecise as it was often difficult to tell where the beginning of the flap was and the flap margins were weakly crenulated in some populations and smooth in others. These counts were considered estimates and not used in the statistical analyses or diagnoses.

Other characters examined were the number of dark, sinuous, bands between limb insertions; the contact or lack thereof between the supranasal scales; presence or absence of an infra-auricular flap; the presence or absence of a supra-auricular lobe as opposed to only a weak ridge or nothing at all; presence or absence of dorsal and caudal tubercles; presence or absence of an emargination (*i.e.,* notch *sec.* Brown, [1999]) between the distal portion of the leading edge of the pre-antebrachial flap and the medial margin of digit I where the flap inserts on the digit as opposed to the pre-antebrachial flap inserting on the digit with no emargination; the presence or absence of prominently raised ridges on the ventral surface of the patagia extending from the body to the outer edge; the presence or absence of enlarged, dorsal, transverse caudal scales forming intermittent whorls; the presence of posteriorly directed (*i.e.,* angling) caudal lobes and whether or not they fuse to form a short, narrow, terminal flap; whether or not the caudal lobes decrease in size posteriorly; edges of caudal flap being smooth or crenulated; presence or absence

of a thick, dark, postorbital stripe; presence or absence of large, irregularly shaped, white vertebral markings; and the presence or absence of distinct black and white subcaudal bands in adults.

Nineteen of the 35 preserved specimens of *Ptychozoon lionotum s.l.* used in this study were not represented in the molecular phylogenetic analyses. An *a priori* decision as to which mitochondrial lineage to group them with prior to additional downstream analyses, was based on their geographic proximity to that lineage. Following this, all individuals (n=44) were then subjected to a Discriminant Function Analysis (DFA) using the MASS Package in R (Ripley *et al.* 2018) based on seven meristic (SU, IL, MB, VS, PS, PPS, TL4) and five scaled (see below) mensural characters (HL, HW, HD, SNL, AXG) to assess the grouping each individual with a particular mitochondrial lineage based on geography. DFA uses linear combinations of untransformed data to characterize and separate predefined groups and explicitly attempts to model the difference between them. The predict() command was used to calculate the posterior probability for lineage membership of each individual. In all but three cases (see below), lineage membership based on geography was correct. For the DFA to generate robust posterior probabilities, however, the sample size (observations) must be greater than the number of characters (variables) and the data should be normally distributed (Chiari & Claude 2012). The latter condition was not met for all characters, however, DFA is less sensitive to non-normally distributed characters than other discriminant analyses. Nonetheless, a second discriminant analysis was performed using the factor loadings from the principal component analysis (see below) as a cross-validation for each individual's lineage membership.

Following Levene's tests for homogeneity of variances (necessary for an analysis of variance [ANOVA] using unequal sample sizes), mitochondrial lineages (*i.e.,* populations) delimited in the phylogeny and the DFA were subjected to ANOVA analyses to ascertain if statistically significant ($p<0.05$) mean differences among the meristic and mensural characters existed. ANOVAs having a *p*-value less than 0.05, indicating that statistical differences existed within the data set, were subjected to a Tukey HSD test to ascertain which character means among which lineage pairs differed significantly.

Characters bearing significantly different means among lineage pairs where subjected to a principal component analysis (PCA) in order to 1) visualize how overall character variation separated lineages from one another in multidimensional space, 2) ascertain which characters contributed most to the overall variation, and 3) determine if their morphospatial relationships coincided with the putative species boundaries delimited by the phylogenetic and GMYC analysis and subsequently defined by the univariate and discrete (presence or absence) character analyses. Using the ADEGENET package in R (Jombart *et al.* 2010), PCA and discriminant analysis of principal components (DAPC) were used on a concatenated meristic and mensural data set. PCA, implemented by the prcomp() command in R, is an indiscriminate analysis that uses the overall character variation among all individuals (*i.e.* data points) while treating each individual independently (*i.e*. not coercing individuals into pre-defined groups) and plots the data points on a multidimensional graph. Mensural characters were scaled to either SVL or head length HL in order to remove any potential effects of allometry. To search for differences in HL and AXG, both were scaled independently for each lineage to SVL using the following equation: Xadj=X-β(SVL-SVLmean), where Xadj=adjusted value; X=measured value; β=unstandardized regression coefficient for each OTU; and SVLmean=overall average SVL of all OTU's (Thorpe, 1975, 1983; Turan, 1999; Lleonart et al. 2000). To assess differences in head shape, HW, HD, and SNL were scaled separately to HL for each population using the equation: Xadj=X-β(HL-HLmean), where Xadj=adjusted value; X=measured value; β=unstandardized regression coefficient for each OTU; and HLmean=overall average HL of all OTU's. All characters used in the PCA were log-transformed and scaled to their standard deviation prior to analysis in order to normalize their distribution so as to ensure characters with very large and very low values did not over-leverage the results owing to intervariable nonlinearity and to insure the data were analyzed on the basis of correlation not covariance. The number of pore-bearing precloacal scales in males was not included in the PCA because sampling across all individuals was incomplete.

In order to determine the number of interpretable PCs (*i.e.*, those that capture the most amount of variation in the data set with the least amount of noise) to retain for downstream analyses prior to PC degeneration (*i.e.*, subsequent PCs represent negligible structure in the data), a modified version of the broken stick model (Cangelosi & Goriely 2007) which uses a stopping rule (Jackson 1993), was implemented with the VEGAN package in R (Oksanen *et al.* 2018) using the bs() command. This analysis produces overlapping curves of eigenvalues and broken stick values and proposes that the number of retained PCs should have eigenvalues higher than their corresponding random broken stick components. For this analysis, PC1 and PC2 which accounted for 54% of the variation in the data set, were retained. Factor loadings from PC1 and PC2 for each population were subjected to an ANOVA in

order to determine which factor loading means between which species pairs differed significantly ($P<0.05$). This method evaluates whether or not each species occupies a statistically different position along PC1 and/or PC2 from other populations, thus enabling a more quantifiable interpretation of the PCA.

Based on the PCA, a DAPC was performed which places the individuals of each predefined population (inferred from the phylogeny and DFA) into separate clusters (*i.e*. plots of points) bearing the smallest within-group variance that produce linear combinations of centroids having the greatest between-group variance (*i.e.* linear distance; Jombart *et al.* 2010). DAPC relies on log transformed and scaled data from the PCA as a prior step to ensure that the variables analyzed are not correlated and number fewer than the sample size. Principal component factor scores generated by the DAPC are plotted in a scree plot and the PCs contributing to at least 90% of the cumulative variation in the data set prior to asymptote are retained for analysis. Retaining too many variables, forces false structure to appear in the data and retaining too few, runs the risk of missing true structure (Cangelosi & Goriely 2007). For this analysis, the first five of the nine PCs were retained which accounted for 97.8% of the variation. To cross-validate the probability of lineage membership for each specimen calculated in the DFA, membership probabilities were calculated based on posteriors retained from the discriminant functions of the DAPC (Jombart *et al.* 2010) using the round(head) command in R v 3.2.1 (R Core Team, 2015).

Museum abbreviations follow Sabaj (2016) except for LSUHC referring to the La Sierra University Herpetological Collection, La Sierra University, Riverside, California, 92505, USA; LSUDPC for La Sierra University Digital Photograph Collection, La Sierra University, Riverside, California, 92505, USA; RMB refers to the field numbers of Rafe M. Brown, Department of Ecology and Evolutionary Biology and Biodiversity Institute, University of Kansas, Lawrence, Kansas USA; JAM refers to the field numbers of Jimmy A. McGuire, Museum of Vertebrate Zoology, University of California, Berkeley, California, USA; and SYS refers to Sun Yat-sen University Museum of Biology, Guangzhou, China.

Results

Both the ML and BI analyses resulted in the same, generally well-supported topology that recovered four deeply divergent, allopatric, mitochondrial clades within *Ptychozoon lionotum s.l.* (Figs. 1, 2). The analyses also recovered *P. lionotum s.l.* as paraphyletic with respect to *P. popaense* in that *P. popaense* is the weakly supported (BI 0.90/UFB 75) sister species of *P. lionotum* populations from Laos, Cambodia, Thailand, and Myanmar to the exclusion of *P. lionotum* from Peninsular Malaysia (*P. cicakterbang* **sp. nov.**, see description below). The latter is the well-supported (1.00/100) sister species to all of these (Fig. 2). Individuals from Thailand, Cambodia, and one from Myanmar (*P. tokehos* **sp. nov.**, see description below) form a well-supported mitochondrial lineage (1.00/100) and range from the Thai-Malay Peninsula in southern Thailand and southern Myanmar, around the Chao Phraya Basin to at least the Cardamom Mountains of southern Cambodia and likely on into southern Vietnam (Figs. 1, 2). This lineage was recovered as the unsupported (0.58/47) closest relative to the well-supported (1.00/100) sister clades from Myanmar and northwestern Laos (*P. lionotum s.s.,* see below) and northeastern Laos (*P. kabkaebin* **sp. nov.**, see description below; Figs. 1, 2). *Ptychozoon lionotum s.s.* is represented by four, essentially genetically identical individuals (Fig. 3) that collectively extend 1,100 km from northwestern Laos through the type locality at Hpa Lon, Yangon Region (see below) to Rakhine State in western Myanmar (Fig. 1) and thus constitute what we hereinafter refer to as *P. lionotum.*

The GMYC species delimitation analysis recovered the same six ingroup mitochondrial clades of the *Ptychozoon lionotum* group recovered by the ML and BI analyses (Fig. 2) with a highly significant likelihood ratio of 61.19726 ($p = 5.140333^{-16}$) and no intra-clade substructuring. Sukumaran & Knowles (2017) demonstrated that the multispecies coalescent generally overestimates species diversity by recovering clades rather than species and that additional criteria such as morphology should be used in conjunction with these analyses. Fujisawa & Barraclough (2013) specifically noted that the GMYC approach should be used in conjunction with additional independent data. We agree with these recommendations and believe the GMYC recovered noteworthy interpopulational genetic structure within the *P. lionotum* group that is corroborated by the statistical morphological and color pattern analyses in that each bears a unique and/or a unique suite of diagnostic characters (see below). Therefore, we hypothesize that these lineages are separate species based on this more integrative approach.

TABLE 3. Summary statistics and principal component analysis scores for *Ptychozoon lionotum, P. cicakterbang* **sp. nov.**, *P. kabkaebin* **sp. nov.**, and *P. tokehos* **sp. nov.** Abbreviations are listed in the Materials and methods.

	PC1	PC2	PC3	PC4	PC5	PC6	PC7	PC8	PC9
Standard deviation	1.663802589	1.454129103	1.07298737	0.928870234	0.816343589	0.740175391	0.590388059	0.563183353	0.472395677
Proportion of Variance	0.30758	0.23494	0.12792	0.09587	0.07405	0.06087	0.03873	0.03524	0.0248
Cumulative Proportion	0.30758	0.54253	0.67045	0.76631	0.84036	0.90123	0.93996	0.9752	1
Eigenvalue	2.768239054	2.114491449	1.151301895	0.862799911	0.666416855	0.54785961	0.34855806	0.317175489	0.223157676
SU	-0.319331301	0.444405009	-0.0480494	0.345637917	-0.310315707	0.009034338	-0.327648213	-0.310303738	0.527956604
IL	-0.413379965	0.352375638	0.124880014	0.087344528	-0.409649551	0.137523991	0.045995682	0.271725224	-0.647339576
MB	-0.140845257	0.354094489	0.599037655	0.072387484	0.545507369	-0.031260344	0.298786296	-0.315936804	-0.055216236
VS	-0.353963495	-0.199543316	0.448929305	-0.437802649	-0.278811548	-0.285171306	0.157126098	0.31016697	0.402160312
TL4	-0.431659792	-0.20250397	0.037110686	-0.238301191	0.390210095	0.499266263	-0.553180821	0.08327423	-0.004792539
HW	-0.159449052	-0.553444402	0.170210511	0.06749668	-0.338465994	0.161249704	0.117013234	-0.668980326	-0.181550006
HD	0.249036969	-0.255990624	0.46431024	0.625739182	-0.069224781	0.291423725	-0.067462303	0.389190185	0.139913706
AXG	-0.428859722	-0.120386521	-0.409708308	0.239357646	0.166091105	0.273095301	0.63292219	0.153459636	0.22388789
SNL	-0.352594291	-0.292920599	-0.088988128	0.407196993	0.247741328	-0.681123007	-0.227434401	0.066100269	-0.186404245

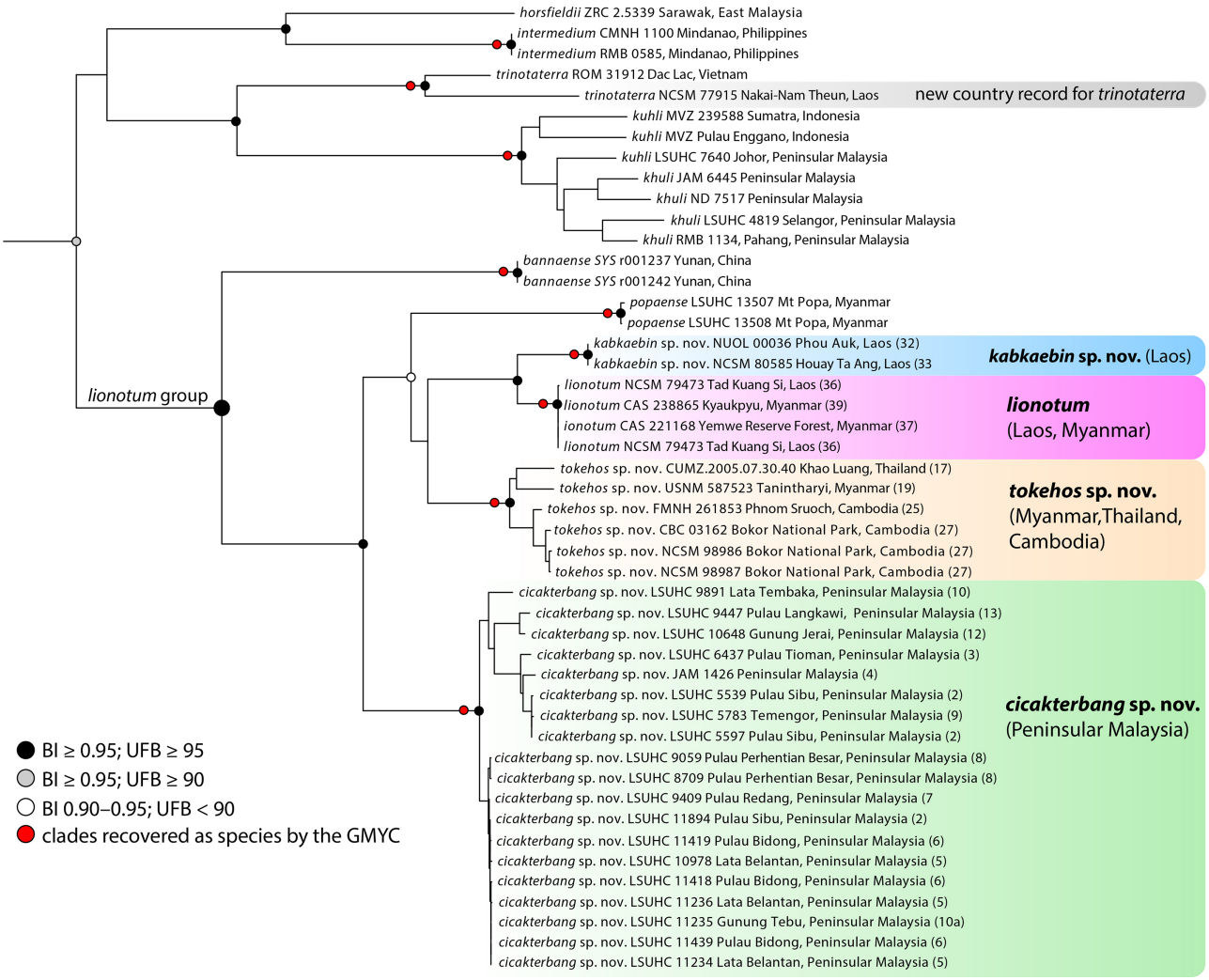

FIGURE 2. Maximum likelihood consensus tree topology depicting the phylogenetic relationships of species within the genus *Ptychozoon*. Numbers in parentheses refer to numbered localities in Figure 1.

The DFA calculated the posterior probabilities for species membership and placed 41 of the 44 individuals into their *a priori* geographically designated species. The posterior probabilities of three individuals did not corroborate their *a priori* species designation. LSUHC 11234 from Lata Belatan, Peninsular Malaysia had a posterior probability of 77.0%, placing it within *P. tokehos* **sp. nov.** instead of *P. cicakterbang* **sp. nov.** (22.8%). However, in the molecular phylogeny, LSUHC 11234 is deeply embedded among other individuals of *P. cicakterbang* **sp. nov.**, including two specimens (LSUHC 10978 and 12236) from Lata Belatan that were collected in the same campground and correctly placed in *P. cicakterbang* **sp. nov.** by the DFA. Additionally, one other specimen (LSUHC 11235) from Lata Belatan (not in the tree) was also correctly assigned. We regard species membership based on the molecular phylogeny to be more robust than that of the DFA and consider LSUHC 11234 to be *P. cicakterbang* **sp. nov.** Another specimen (FMNH 261853) from the Cardamom Mountains, Cambodia was assigned to *P. lionotum* (49.1%) by the DFA as opposed to *P. tokehos* **sp. nov.** (17.6%). We consider this to also be erroneous as other specimens from the Cardamom Mountains in the phylogeny (CBC 03162, and NCSM 98986–87) and others not in the phylogeny (FMNH 261852–54 and CBC 01217) were all correctly placed in *P. tokehos* **sp. nov.** The DFA placed FMNH 177548 from Chiang Mai, Thailand in *P. tokehos* **sp. nov.** with a 76.3% probability (Fig. 4). However, the closest population of *P. tokehos* **sp. nov.** represented in the phylogeny lies approximately 760 km to the south in the Cardamom Mountains (Fig. 1). Geographically intervening specimens from Sakaerat (FMNH 18123–24, 18128–29, 181844) that were not represented in the tree were also placed in *P. tokehos* **sp. nov.** Based on geographic proximity, FMNH 177548 was placed *a priori* in *P. lionotum* but the probability of that being correct based on the DFA was very low (6.64^{-06}%). A cross-validation of species membership using posteriors retained from the discriminant

functions of the DAPC corroborated the DFA and placed FMNH 177548 in *P. tokehos* **sp. nov.** with a 78.2% probability. Unfortunately, FMNH 177548 has a regenerated tail precluding the evaluation of discrete diagnostic caudal characters that could potentially differentiate *P. tokehos* **sp. nov.** from *P. lionotum*. In the absence of competing data other than geography, we provisionally consider FMNH 177548 as part of *P. tokehos* **sp. nov.** (Fig. 4). Unequivocal resolution of the specific identity and phylogenetic placement of this population must await the acquisition of additional specimens and molecular data.

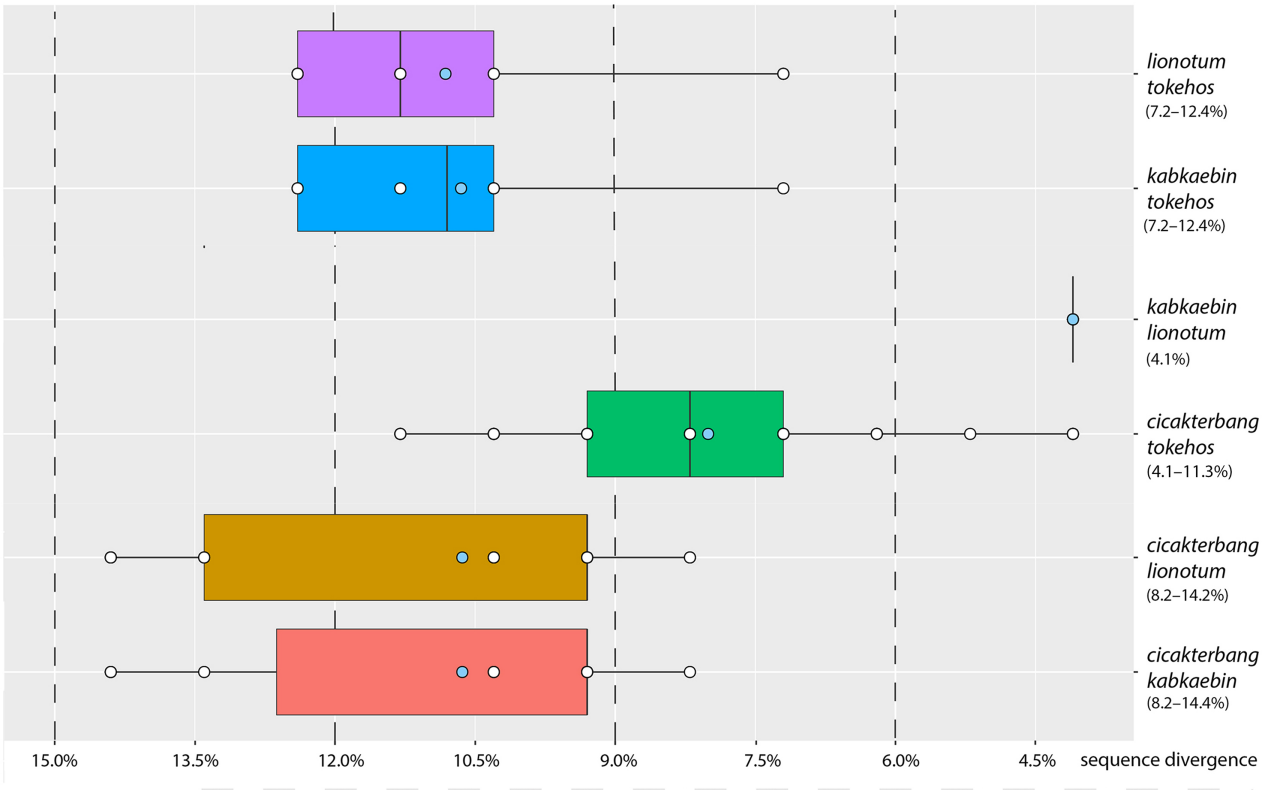

Ranges of Uncorrected Pairwise Sequence Divergences

	1	2	3	4	5	6	7	8	9	10	11	12	13	14	15	16	17	18	19	20	21	22	23	24	25	26	27	28	29	30	31	32	33	34	35
1. *bannaense SYS* r001237	0.000																																		
2. *bannaense* SYS r001242	0.000	0.000																																	
3. *cicakterbang* LSUHC 9059	0.093	0.093	0.000																																
4. *cicakterbang* LSUHC 8709	0.093	0.093	0.000	0.000																															
5. *cicakterbang* LSUHC 9409	0.093	0.093	0.000	0.000	0.000																														
6. *cicakterbang* LSUHC 11419	0.093	0.093	0.000	0.000	0.000	0.000																													
7. *cicakterbang* LSUHC 11418	0.093	0.093	0.000	0.000	0.000	0.000	0.000																												
8. *cicakterbang* LSUHC 11439	0.093	0.093	0.000	0.000	0.000	0.000	0.000	0.000																											
9. cicakterbang LSUHC 9891	0.124	0.124	0.031	0.031	0.031	0.031	0.031	0.031	0.000																										
10. *cicakterbang* LSUHC 10978	0.103	0.103	0.010	0.010	0.010	0.010	0.010	0.010	0.041	0.000																									
11. *cicakterbang* LSUHC 11234	0.093	0.093	0.000	0.000	0.000	0.000	0.000	0.000	0.031	0.010	0.000																								
12. *cicakterbang* LSUHC 11236	0.093	0.093	0.000	0.000	0.000	0.000	0.000	0.000	0.031	0.010	0.000	0.000																							
13. *cicakterbang* LSUHC 11235	0.093	0.093	0.000	0.000	0.000	0.000	0.000	0.000	0.031	0.010	0.000	0.000	0.000																						
14. *cicakterbang* LSUHC 5783	0.103	0.103	0.072	0.072	0.072	0.072	0.072	0.072	0.082	0.062	0.072	0.072	0.072	0.000																					
15. *cicakterbang* LSUHC 9447	0.124	0.124	0.031	0.031	0.031	0.031	0.031	0.031	0.062	0.041	0.031	0.031	0.031	0.082	0.000																				
16. *cicakterbang* LSUHC 10648	0.113	0.113	0.021	0.021	0.021	0.021	0.021	0.021	0.052	0.031	0.021	0.021	0.021	0.072	0.010	0.000																			
17. *cicakterbang* JAM 1426	0.103	0.103	0.072	0.072	0.072	0.072	0.072	0.072	0.082	0.062	0.072	0.072	0.072	0.000	0.082	0.072	0.000																		
18. *cicakterbang* LSUHC 6437	0.103	0.103	0.072	0.072	0.072	0.072	0.072	0.072	0.082	0.062	0.072	0.072	0.072	0.000	0.082	0.072	0.000	0.000																	
19. *cicakterbang* LSUHC 11894	0.093	0.093	0.000	0.000	0.000	0.000	0.000	0.000	0.031	0.010	0.000	0.000	0.000	0.072	0.031	0.021	0.072	0.072	0.000																
20. *cicakterbang* LSUHC 5539	0.113	0.113	0.082	0.082	0.082	0.082	0.082	0.082	0.093	0.072	0.082	0.082	0.082	0.010	0.093	0.082	0.010	0.010	0.082	0.000															
21. *cicakterbang* LSUHC 5597	0.103	0.103	0.072	0.072	0.072	0.072	0.072	0.072	0.082	0.062	0.072	0.072	0.072	0.000	0.082	0.072	0.000	0.000	0.072	0.010	0.000														
22. *kabkaebin* NUOL 00036	0.144	0.144	0.093	0.093	0.093	0.093	0.093	0.093	0.103	0.103	0.093	0.093	0.093	0.144	0.093	0.082	0.144	0.144	0.093	0.134	0.144	0.000													
23. *kabkaebin* NCSM 80585	0.144	0.144	0.093	0.093	0.093	0.093	0.093	0.093	0.103	0.103	0.093	0.093	0.093	0.144	0.093	0.082	0.144	0.144	0.093	0.134	0.144	0.000	0.000												
24. *lionotum* CAS 221168	0.144	0.144	0.093	0.093	0.093	0.093	0.093	0.093	0.103	0.103	0.093	0.093	0.093	0.144	0.093	0.082	0.144	0.144	0.093	0.134	0.144	0.041	0.041	0.000											
25. *lionotum* CAS 238865	0.144	0.144	0.093	0.093	0.093	0.093	0.093	0.093	0.103	0.103	0.093	0.093	0.093	0.144	0.093	0.082	0.144	0.144	0.093	0.134	0.144	0.041	0.041	0.000	0.000										
26. *lionotum* NCSM 79474	0.144	0.144	0.093	0.093	0.093	0.093	0.093	0.093	0.103	0.103	0.093	0.093	0.093	0.144	0.093	0.082	0.144	0.144	0.093	0.134	0.144	0.041	0.041	0.000	0.000	0.000									
27. *lionotum* NCSM 79473	0.144	0.144	0.093	0.093	0.093	0.093	0.093	0.093	0.103	0.103	0.093	0.093	0.093	0.144	0.093	0.082	0.144	0.144	0.093	0.134	0.144	0.041	0.041	0.000	0.000	0.000	0.000								
28. *popaense* LSUHC 13507	0.155	0.155	0.113	0.113	0.113	0.113	0.113	0.113	0.144	0.124	0.113	0.113	0.113	0.124	0.113	0.103	0.124	0.124	0.113	0.113	0.124	0.134	0.134	0.134	0.134	0.134	0.134	0.000							
29. *popaense* LSUHC 13508	0.155	0.155	0.113	0.113	0.113	0.113	0.113	0.113	0.144	0.124	0.113	0.113	0.113	0.124	0.113	0.103	0.124	0.124	0.113	0.113	0.124	0.134	0.134	0.134	0.134	0.134	0.134	0.021	0.000						
30. *tokehos* DSM 798	0.103	0.103	0.041	0.041	0.041	0.041	0.041	0.041	0.072	0.052	0.041	0.041	0.041	0.093	0.062	0.052	0.093	0.093	0.041	0.082	0.093	0.072	0.072	0.072	0.072	0.072	0.072	0.093	0.093	0.000					
31. *tokehos USNM 587523*	0.134	0.134	0.072	0.072	0.072	0.072	0.072	0.072	0.082	0.072	0.072	0.072	0.072	0.103	0.093	0.082	0.103	0.103	0.072	0.113	0.103	0.103	0.103	0.113	0.113	0.113	0.113	0.134	0.144	0.052	0.000				
32. *tokehos* FMNH 261852	0.124	0.124	0.062	0.062	0.062	0.062	0.062	0.062	0.072	0.072	0.062	0.062	0.062	0.093	0.082	0.072	0.093	0.093	0.062	0.082	0.093	0.103	0.103	0.103	0.103	0.103	0.103	0.093	0.103	0.031	0.041	0.000			
33. *tokehos* CBC 03162	0.134	0.134	0.082	0.082	0.082	0.082	0.082	0.082	0.093	0.093	0.082	0.082	0.082	0.113	0.103	0.093	0.113	0.113	0.082	0.103	0.113	0.124	0.124	0.124	0.124	0.124	0.124	0.103	0.113	0.052	0.062	0.021	0.000		
34. *tokehos* NCSM 98986	0.134	0.134	0.072	0.072	0.072	0.072	0.072	0.072	0.082	0.082	0.072	0.072	0.072	0.103	0.093	0.082	0.103	0.103	0.072	0.093	0.103	0.113	0.113	0.113	0.113	0.113	0.113	0.103	0.113	0.041	0.052	0.010	0.010	0.000	
35. *tokehos* NCSM 98987	0.134	0.134	0.082	0.082	0.082	0.082	0.082	0.082	0.093	0.093	0.082	0.082	0.082	0.113	0.103	0.093	0.113	0.113	0.082	0.103	0.113	0.124	0.124	0.124	0.124	0.124	0.124	0.103	0.113	0.052	0.062	0.021	0.000	0.010	0.000

FIGURE 3. Uncorrected pairwise sequence divergence between species of rhe *Ptychzoon lionotum* group (boxplots) and between individuals of the *P. lionotum* group (matrix). Colored squares represent the 50% quartile. Light-blue circles are means.

The species lineages delimited by the phylogenetic analyses and the DFA are corroborated by additional analyses. The ANOVA identified nine of the 12 selected meristic and mensural characters as bearing significantly different mean values between one or more pairs of species (Fig. 5) and further indicated that each species is significantly different from every other species in at least one character mean. All species except *P. kabkaebin* **sp. nov.** and *P. tokehos* **sp. nov.** were well-separated in the PCA along the combined ordination of the first three PCs which accounted for 67.0% (Table 3) of the variation in the data (Fig. 6). PC1 accounted for 30.7% of the variation and loaded most heavily for axilla-groin length (AXG) and fourth toe lamellae (TL4). PC2 accounted for 23.5% of

the variation and loaded most heavily for head width (HW). Lastly, PC3 accounted for an additional 12.8% of the variation and loaded most heavily for the number of midbody scales (MB). ANOVA analyses of the factor loadings of PC1 among the four species indicated that the mean values between the species pairs of *P. cicakterbang* **sp. nov.** and *P. kabkaebin* **sp. nov.** and *P. cicakterbang* **sp. nov.** and *P. tokehos* **sp. nov.** were highly significantly different (p=0.0003 and p=1.26^{-07}, respectively), indicating that *P. cicakterbang* **sp. nov.** occupies a significantly different position along PC1 than the either of the other two species (Fig. 6). ANOVA analyses of the factor loadings of PC2 means were significantly different between the species pairs of *P. cicakterbang* **sp. nov.** and *P. lionotum* (p=2.65^{-06}), *P. tokehos* **sp. nov.** and *P. kabkaebin* **sp. nov.** (p=0.49), and *P. tokehos* **sp. nov.** and *P. lionotum* (p=1.71^{-06}), indicating that *P. tokehos* **sp. nov.** occupies a significantly different position than *P. kabkaebin* **sp. nov.** and *P. lionotum* along PC2 and *P. cicakterbang* **sp. nov.** differs significantly in position from *P. lionotum* along PC2 (Fig. 6). The DAPC revealed clear separation among the four species with complete separation of the 95% confidence ellipses among all species (Fig. 6).

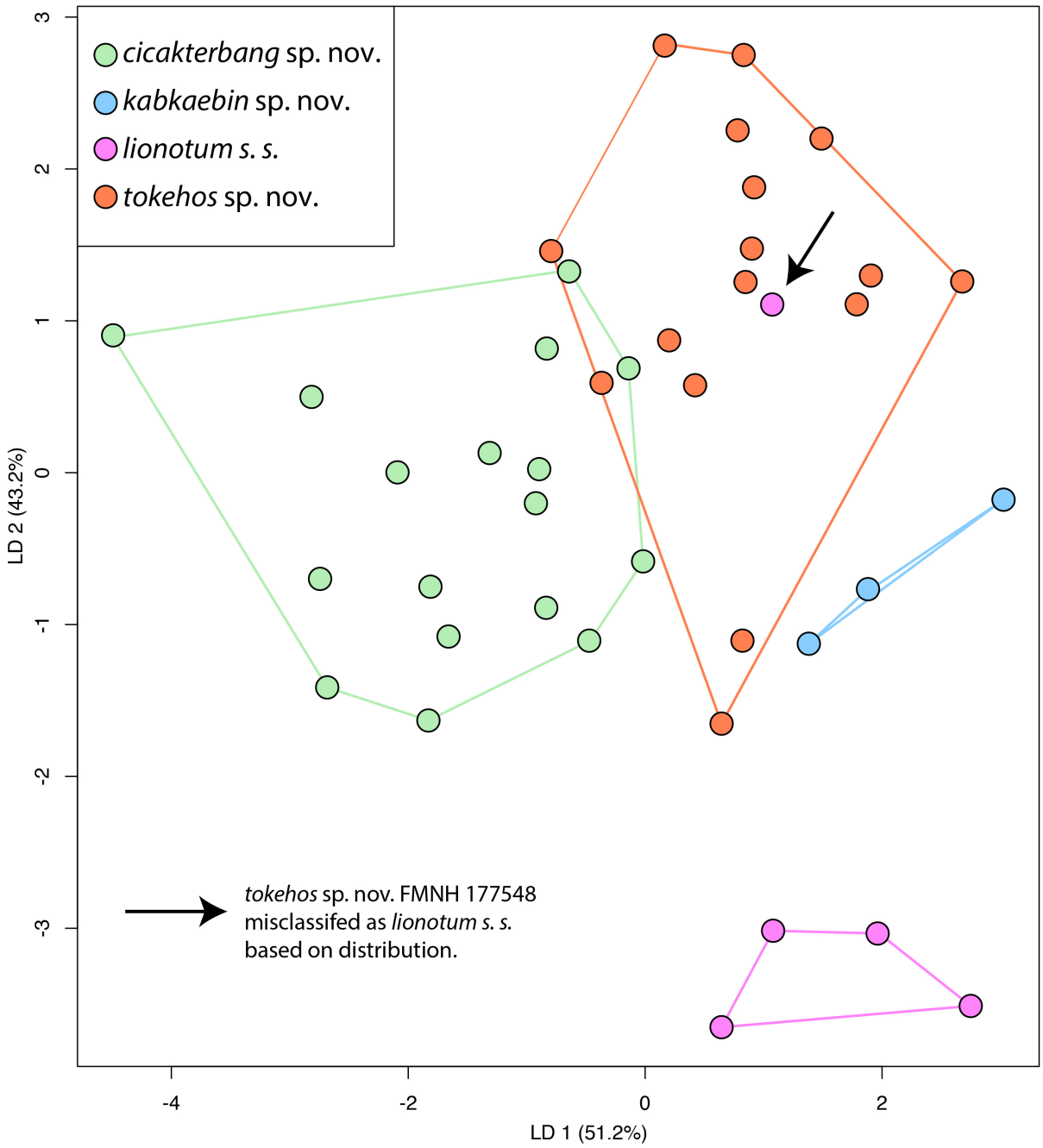

FIGURE 4. Discriminant function analysis showing the separation of *P. lionotum s.s.*, *P. cicakterbang* **sp. nov.**, *P. kabkaebin* **sp. nov.**, and *P. tokehos* **sp. nov.** and the misplacement of FMNH 177548 as *P. lionotum*.

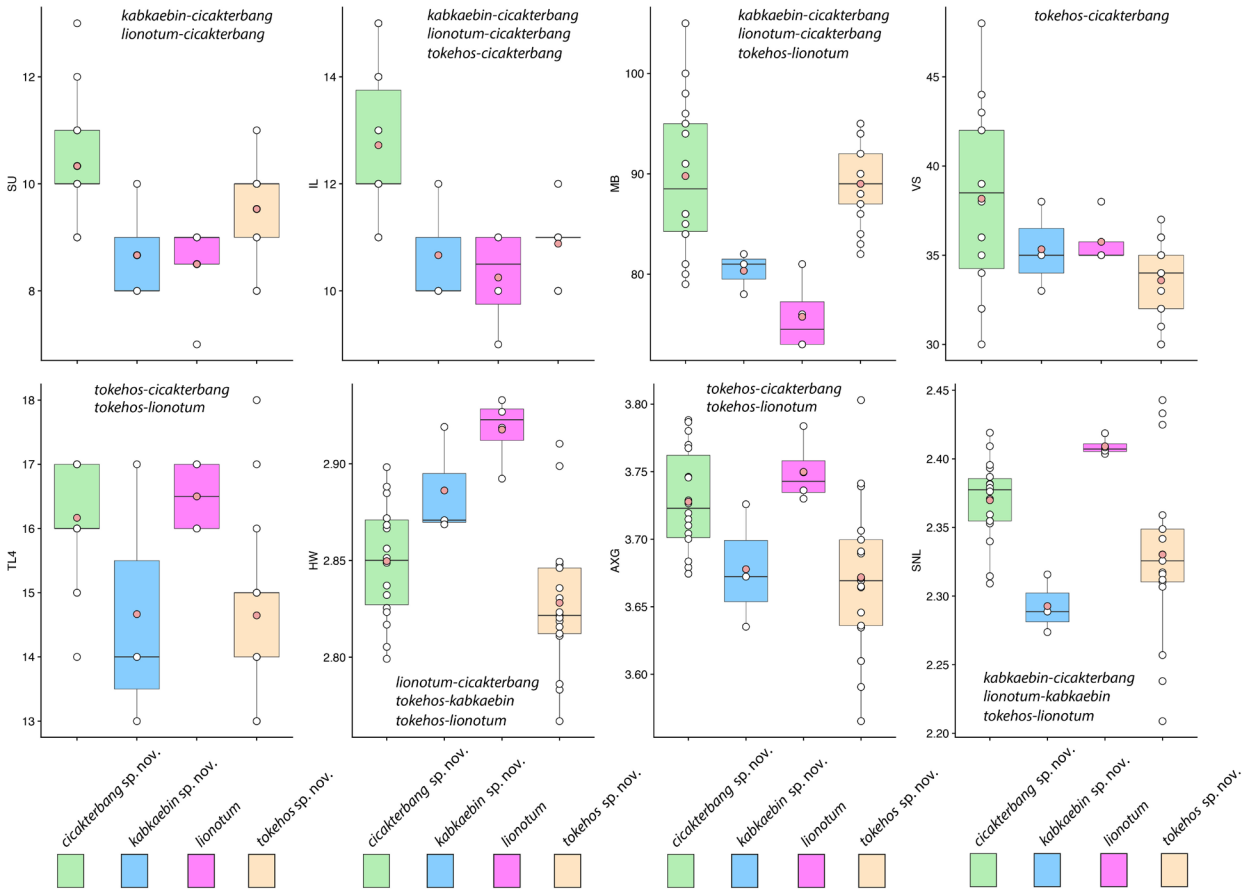

FIGURE 5. Boxplot analyses of the characters bearing statistically significant mean values between various combinations of species pairs. The species pairs are listed on the plot. Colored squares represent the 50% quartile. Orange circles are the means.

We are well aware that mtDNA phylogenies can reveal significant structure in a data set by recovering sequentially nested monophyletic groups even though within that same data set, nuclear genes can indicate significant gene flow among these groups (*e.g.* Shaw 2002; Fisher-Reid & Wiens 2011; Toews & Brelsford 2012), thus precluding their species status. This weakens any hypothesis of specific identity based *solely* on mtDNA data. Given the phylogenetic relationships of the four allopatric species that bear deep genetic divergences among them (4.1–14.5%; Fig. 3), the statistically significant differences between the factor loading means of PC1 and PC2, the statistically significant mean differences of five meristic and three scaled mensural characters (Fig. 5), and discrete differences in morphological and color pattern characters (Table 4) in varying species combinations, we regard their separate specific identities as robust, testable hypotheses.

Taxonomy

Ptychozoon cicakterbang sp. nov.
Malaysia Parachute Gecko
Figs. 7, 8

Ptychozoon homalocephalum Cantor, 1847:626 (in part); Boulenger, 1912:52 (in part)
Ptychozoon kuhli Smith, 1935:119 (in part)
Ptychozoon lionotum Manthey & Grossmann, 1997:247 (in part); Cox *et al.,* 1998:81 (in part); Das, Dattagupta, & Gayen, 1998:131 (in part); Chan-ard *et al.,* 1999:132 (in part); Kluge, 2001:25 (in part); Leong *et al.,* 2003:170; Grismer, 2011a:532, 2011b:139; Grismer *et al.,* 2011:78 (in part); Grismer *et al.,* 2018a:203 (in part).
Ptychozoon lionatum (sic.) Grismer, Youmans, Wood, & Grismer 2006:161;Grismer & Pan, 2008:278.

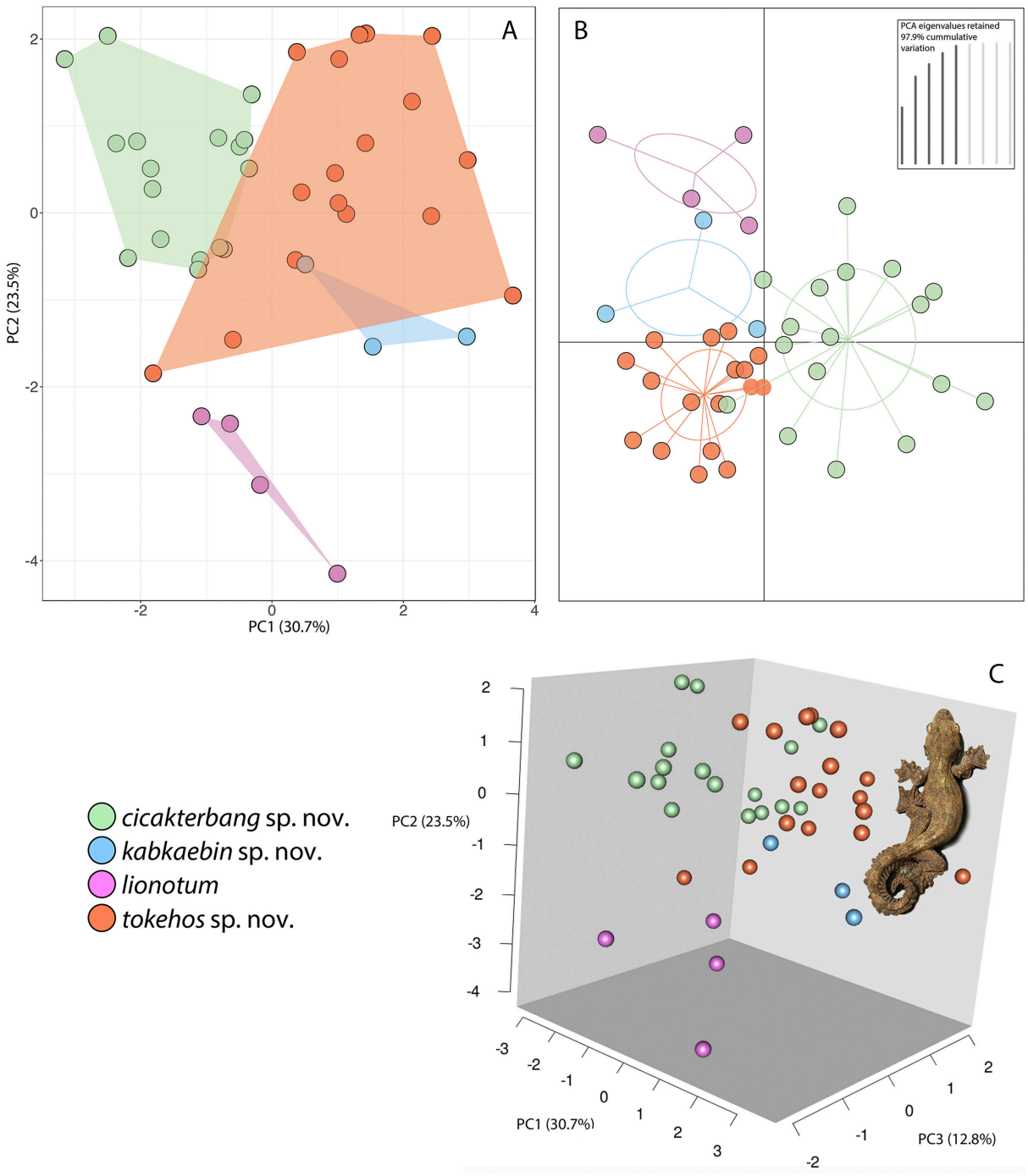

FIGURE 6. Multivariate analyses of *P. lionotum*, *P. cicakterbang* **sp. nov.**, *P. kabkaebin* **sp. nov.**, and *P. tokehos* **sp. nov.** A. PCA ordination along PC 1 and PC2. B. DAPC showing complete separation of the 95% confidence ellipses. C. PCA ordination along PC1, PC2, and PC3.

Holotype. LSUHC 10648 adult female collected by Evan S. H. Quah, L. Lee Grismer, Anuar Shahrul, and Jesse L. Grismer on 26 June 2012 on the road to the top of Gunung Jerai, Kedah, Peninsular Malaysia (5.8099°N, 100.4367°E, 744 m above sea level).

Paratypes. LSUHC 5597 adult male collected by Jesse L. Grismer, L. Lee Grismer, and Perry L. Wood Jr. on 23 July 2003 from Pulau Sibui, Johor, Peninsular Malaysia (2.217539°N, 104.069966°E, 16 m above sea level). LSUHC 5783 bears the same data as LUSHC 5597 except it was collected on 1 September 2003. LSUHC 8709 adult male collected by L. Lee Grismer, Perry L. Wood Jr., and Jesse L. Grismer from Pulau Perhentian Besar,

Terengganu, Peninsular Malaysia (5.901514°N, 102.746672°E, 123 m above sea level). LSUHC 9059 adult female bearing the same collection data as LSUHC 8709 except being collected on 18 October 2007. LSUHC 9447 adult female collected by Perry L. Wood Jr., Jesse L. Grismer, and L. Lee Grismer from Gunung Machinchang, Pulau Langkawi, Kedah, Peninsular Malaysia (6.386111°N, 99.661111°E, 634 m above sea level). LSUHC 10978 adult female collected by Evan S. H. Quah and L. Lee Grismer on 7 September 2013 from Hutan Lipur Lata Belatan, Terengganu, Peninsular Malaysia (5.579567°N, 102.589028°E, 527 m above sea level). LSUHC 11058 adult female collected by L. Lee Grismer and Shahrul Anuar on 26 June 2013 from Kem Baha, Gunung Stone, Kelantan, Peninsular Malaysia (5.340092°N, 101.966917°E, 511 m above sea level). LSUHC 11418 adult male collected by Evan S. H. Quah and L. Lee Grismer on 26 June 2013 from Pulau Bidong, Terengganu, Peninsular Malaysia (5.620990°N, 103.058062°E, 25 m above sea level).

FIGURE 7. Holotype of *Ptychozoon cicakterbang* **sp. nov.** LSUHC 10648 from Gunung Jerai, Kedah, Peninsular Malaysia. Photograph by L. L. Grismer.

Additional specimens examined. LSUHC 5539 adult female collected by Jesse L. Grismer, L. Lee Grismer, Perry L. Wood Jr. on 23 July 2003 from Pulau Sibu, Johor, Peninsular Malaysia (2.21754°N, 104.06997°E, 16 m above sea level); LSUHC 6437 adult female collected by Jesse L. Grismer and Perry L. Wood Jr. on 2 July 2004 from the Tekek-Juara Trail, Pulau Tioman, Pahang, Peninsular Malaysia (2.82070°N, 104.168954°E, 110 m above sea level); LSUHC 9409 adult female collected by Evan S. H. Quah and L. Lee Grismer at the Reng Reef field station, Pulau Redang, Terengganu, Peninsular Malaysia (5.81212°N, 103.000749°E, 49 m above sea level); LSUHC 9891 adult female collected by Perry L. Wood Jr., L. Lee Grismer, and Jesse L. Grismer on 6 September 2007 from Lata Tembaka, Terengganu, Peninsular Malaysia (5.554063°N, 102.431311°E, 690 m above sea level); LSUHC 11439 adult female collected by Evan S. H. Quah and L. Lee Grismer on 26 June 2013 from Pulau Bidong, Terengganu, Peninsular Malaysia (5.620990°N, 103.058062°E, 25 m above sea level). LSUHC 11234–36 collected by Evan S. H. Quah and L. Lee Grismer on 3 July 2013 from Hutan Lipur Lata Belatan, Terengganu, Peninsular Malaysia (5.57957°N, 102.58902°E, 527 m above sea level).

Diagnosis. *Ptychozoon cicakterbang* **sp. nov.** differs from all other species of *Ptychozoon* by having the following unique combination of characters: a maximum SVL of 93.4 mm; supranasals not in contact; 9–13 supralabials; 11–15 infralabials; infra-auricular cutaneous flap present; prominent supra-auricular lobe; no dorsal or caudal tu-

bercles; imbricate parachute support scales on dorsal surface of patagia; raised, prominent ridges on ventral surface of patagia; 79–105 midbody dorsal scales; 30–48 ventral scales; pre-antebrachial flap not inserting on the full length of digit V but leaving a space between them; no enlarged femoral scales; 17–25 pore-bearing precloacal scales in males; 18–28 enlarged precloacal scales; 5–8 rows of enlarged post-precloacal scales; 14–17 transverse subdigital lamellae on the fourth toe; 25–34 scales across the widest portion of the caudal flap; enlarged dorsal caudal scales forming intermittent whorls; distal caudal lobes fusing to form a narrow caudal flap; edges of caudal flap weakly crenulated; caudal lobes angled posteriorly; caudal lobes decrease posteriorly in size; no thick, dark, postorbital stripe; four dark body bands between limb insertions; no irregularly shaped, white, vertebral markings; and subcaudal region banded in adults (Tables 4, 5).

FIGURE 8. Color pattern variation in *Ptychozoon cicakterbang* **sp. nov.** A. LSUHC 9059 from Pulau Perhentian Besar, Terengganu, Peninsular Malaysia. B. LSUHC 8709 from Pulau Perhentian Besar, Terengganu, Peninsular Malaysia. C. LSUDPC 3207 from Butterfly Park at Cameron Highlands, Pahang, Peninsular Malaysia. D. LSUHC 5539 from Pulau Sibu, Johor, Peninsular Malaysia.

TABLE 4. Summary statistics and diagnostic characters among *Ptychozoon lionotum*, *P. cicakterbang* **sp. nov.**, *P. kabkaebin* **sp. nov.**, and *P. tokehos* **sp. nov.** SD = standard deviation and N = sample size.

	P. lionotum	*P. cicakterbang* **sp. nov.**	*P. kabkaebin* **sp. nov.**	*P. tokehos* **sp. nov.**
supralabials to middle of eyeball (SU)				
mean (±SD)	8.5 (±1.00)	10.3 (±1.08)	8.7 (±1.15)	9.5 (±0.87)
range	7–9	9–13	8–10	8–11
N	4	18	3	19
infralabials (IL)				
mean (±SD)	10.3 (±0.96)	12.7 (±1.23)	10.7 (±1.15)	10.9 (±0.60)
range	9–11	11–15	10–12	10–12
N	4	18	3	17
transverse midbody dorsal scales (MB)				
mean (±SD)	75.8 (±3.78)	89.8 (±7.43)	80.3 (±2.08)	89.0 (±4.04)
range	73–81	79–105	78–82	82–95
N	4	18	3	19
ventral scales (VS)				
mean (±SD)	35.8 (±1.50)	38.2 (±4.95)	35.3 (±2.51)	33.6 (±2.35)
range	35–38	30–48	33–38	30–37
N	4	18	3	19
enlarged pore-bearing precloacal scales in males (PP)				
mean (±SD)	21.0 (±1.0)	21.0 (±3.25)	21.0 (±0.00)	21.4 (±1.51)
range	20–22	17–25	21	20–24
N	2	4	1	8
enlarged precloacal scales (PS)				
mean (±SD)	23.8 (±0.50)	22.8 (±2.65)	22.0 (±0.82)	21.8 (±1.91)
range	23 or 24	18–28	22–23	18–25
N	4	18	3	19
enlarged post-precloacal scale rows (PPS)				
mean (±SD)	5.0 (±0.00)	5.9 (±0.99)	6.0 (±0.82)	5.28 (±0.75)
range	5	5–8	5–7	4–7
N	4	18	3	19
transversely expanded 4th toe lamellae (TL4)				
mean (±SD)	16.5 (±0.58)	16.2 (±0.86)	14.6 (±2.08)	14.6 (±1.41)
range	16 or 17	14–17	13–17	13–18
N	4	18	3	19
scales across widest portion of caudal flap (CF)				
mean (±SD)	31.5 (±2.5)	29.1 (±3.27)	28.3 (±1.53)	31.6 (±2.59)
range	29–34	25–34	27–30	28–34
N	2	14	3	11
supra-auricular lobe	weak ridge	prominent lobe	weak ridge	weak ridge
prominent ridges on ventral surface of body flap	no	yes	no	yes
edges of caudal flap	smooth	weakly crenulated	weakly crenulated	smooth
caudal whorls bearing enlarged scales	weak to absent	present	absent	present
thick dark, postorbital stripe	variable	absent	present	variable
irregularly shaped, white vertebral markings	variable	absent	variable	variable
maximum SVL (mm)	95.9	93.4	89.1	97.5

TABLE 5. Character states differentiating species of *Ptychozoon* from one another. Data in part come from Annandale (1905), Brown *et al*. (1997), Brown (1999), Sumontha *et al*. (2012) and Wang *et al*. (2016). / = data unavailable or the character does not exist.

	cicakterbang **sp. nov.**	*kabkaebin* **sp. nov.**	*tokehos* **sp. nov.**	*popaense*	*bamnaense*	*horsfieldii*	*intermedium*	*kuhli*	*lionotum*	*nicobarense*	*rhacophorus*	*trinotaterra*	*kaengkracha-nense*
max SVL (mm)	93.4	95.4	97.5	86.2	87.5	73.9	98.8	107.8	95.9	100.3	64.5	71.3	86
supranasals in contact	no	no	no	no	no	no	yes, no	yes, no	no	yes	no	yes	yes
infra-auricular cutaneous flap	present	present	present	present	present	present	present	present	present	present	absent	present	present
prominent infra-auricular cutaneous lobe	present	absent	absent	absent	absent	absent	absent	absent	absent	absent	absent	absent	absent
disposition of dorsal tubercles	absent	absent	absent	absent	absent or only on occiput	absent	0–10 irregular rows	2–6 straight rows	absent	absent	6–10 rows, scattered	0 or 1 mid-dorsal row	absent
dorsal tubercle shape	absent	absent	absent	absent	flat when present	absent	flat to convex	convex or spiculate	absent	absent	spiculate to highly spinose	flat	absent
enlarged, dorsal parachute support scales	present	present	present	present	present	present	present	present	present	present	absent	present	present
space between pre-antebrachial flap and digit I	present	present	present	present	absent	absent	absent	absent	present	absent	absent	absent	absent
enlarged femoral scales	absent	absent	absent	absent	absent	8–11	12–19	absent	absent	absent	absent	absent	absent
enlarged pore-bearing precloacals in males	17–25	21	20–24	21	17	10–11	8–12	14–32	20–22	14–22	12–18	19–21	14–19
fourth toe lamellae	14–17	13–17	13–18	13 or 14	16 or 17	11–13	9–14	12–16	16 or 17	13–21	11–13	12–14	15–17
scales across widest portion of caudal flap	25–34	27–30	28–34	28 or 29	15	9–21	14–18	42–51	29–34	20–29	/	26	/
distal lobes fused into narrow or wide caudal flap	narrow	narrow	narrow	narrow	narrow	narrow	narrow	wide	narrow	wide	narrow	narrow	narrow
caudal tubercles continue to tail terminus	absent	absent	absent	absent	absent	absent	variably	yes	absent	absent	absent	yes	absent
caudal lobes angled posteriorly	slight	slight	slight	slight	extreme	extreme	extreme	slight	slight	slight	extreme	slight	slight
tail and lobes bearing distal reduction	minimal	minimal	minimal	minimal	extensive	extensive	extensive	minimal	minimal	minimal	extensive	minimal	extensive
thick postorbital stripe	absent	present	variable	present	present	present	present	present	variable	absent	absent	present	absent
bands between limb insertions	4	4	4	4	4	4	3	4	4	3	0	3	3
irregularly shaped, white vertebral markings	absent	variable	variable	present	absent	absent	absent	absent	variable	present	present	present	absent

Description of holotype. Adult female SVL 86.0 mm; head moderate (HL/SVL 0.27), wide (HW/HL 0.76), depressed (HD/HL 0.40), distinct from neck; snout rounded at tip in dorsal profile; prefrontal region concave; lores rounded; rostral scale large, rectangular, bearing an inverted Y-shaped, dorsomedial groove, in contact posteriorly with two supranasals, one postnasal, dorsolaterally with nostrils, and laterally with first supralabials; supralabials (10R,L) to mid-orbital position; infralabials (12R,14L); nostrils elliptical with long axes oriented dorsoventrally, occupying anterior portion of nasal scale, bordered anteriorly by rostral, dorsally by supranasal, posteriorly by four postnasals of varying sizes (upper largest), and ventrally by first and second supralabials; scales on rostrum granular slightly larger than granular scales on top of head and occiput; eyes large (ED/HL 0.22), less than snout length; pupil vertically elliptical, crenelated; supraciliaries elongate, posteriormost weakly pointed; auricular opening rounded, bearing a prominent supra-auricular lobe; tympanum deeply sunk; infra-auricular flap broad, rounded, extending from below corner of mouth to lateral margin of neck midway between posterior margin of ear opening and forelimb insertion, measuring 3.9 mm at its widest point; dorsal scales of infra-auricular flap large, subimbricate proximally, small juxtaposed distally, ventral flap scales minute and granular; mental triangular, slightly wider than deep, bordered laterally by first infralabials and posteriorly by paired, rectangular postmentals contacting medially for 80% of their length; one row of enlarged sublabials bordering infralabials, anteriormost largest; gular scales small, rounded, grading into larger, imbricating throat and subimbricate pectoral and ventral scales.

Body dorsoventrally depressed, relatively stout (AXG/SVL 0.46); patagium 9.4 mm at midpoint of body, bearing enlarged subimbricate, rectangular scales dorsally, minute juxtaposed, subrectangular scales ventrally, ventral surface bearing raised ridges of granular scales extending from body to edge of flap; 86 minute, flat, round, juxtaposed midbody dorsal scales, largest mid-dorsally; four (L) and one (R) large, flat, isolated, dorsal scale(s) immediately anterior to the hind limb insertions; 42 transverse rows of large, smooth, flat, subimbricate ventrals, ventrals much larger than dorsals, decreasing in size laterally into granular scales at base of flap; 23 enlarged, precloacal scales; five rows of enlarged, post-precloacal scales; and scales immediately anterior to vent granular.

Limbs short, robust (FL/SVL 0.11; TBL/SVL 0.15); dorsal scales of forelimbs, flat, juxtaposed, larger than dorsal body scales; ventral forelimb scales subimbricate; anterior and posterior margins of forelimbs, and posterior margins of hind limbs bearing wide, cutaneous flaps; that of anterior margin of forearm (*i.e.* pre-antebrachial flap) emarginated distally and terminating low on base of digit I; scales of forelimb flap large, elongate, subimbricate; those of hind limb flap much smaller, rounded, subimbricate; palmar scales smooth, rounded; digits fully webbed, relatively short, dorsoventrally compressed; undivided transverse subdigital lamellae number 12 (I), 15 (II), 18 (III), 17 (IV), 18 (V), distalmost lamellae V-shaped; claws arise from within the dorsal surface of digital pads; claw of digit I replaced by an enlarged, flat scale; dorsal scales of hind limbs, flat, juxtaposed, larger than dorsal body scales; ventral scales of hind limbs flat, subimbricate, smaller than ventral scales of belly; flat scales of anterior margin of thigh subimbricate; plantar scales smooth, subimbricate; digits fully webbed; transverse subdigital lamellae number 10 (I), 13 (II), 17 (III), 17 (IV), 14 (V), distalmost lamellae V-shaped; claws arise from within the dorsal surface of digital pads; and claw of digit I replaced by an enlarged, flat scale.

Tail original, flattened, shorter than SVL (TL/SVL 0.88); two median rows of transversely widened, smooth subcaudals anteriorly becoming less regular and broken up posteriorly; postcloacal scales large, flat, imbricate; dorsal caudals flat, juxtaposed, larger than dorsal body scales; 6–10 smaller scales between much larger, transversely aligned scales composing whorls; tail width and caudal lobes decrease posteriorly; 23 caudal lobes on each side slightly angled posteriorly; and tail terminates in a short, narrow, flap (7.3 mm) bearing weakly crenulated edges.

Light phase coloration and pattern in life (Fig. 7). Dorsal ground color of head, body, and tail beige; top of head essentially unicolor; labial scales lighter than body, delimited by thin, dark lines at their junctures; infra-auricular flap same lighter color as labial scales; four faint, thin, sinuous dorsal bands between limb insertions transitioning into approximately six darker caudal bands; terminal caudal band on caudal flap nearly black, edged posteriorly by narrow white band; subcaudal region mottled, weakly banded; iris deep-red; gular region, throat, ventral surfaces of forelimbs, pectoral region, and anterior portion of belly dull-white with stippled scales; and posterior margin of belly dull-white, immaculate; stippling on ventral surfaces of hind limbs dense.

Variation (Fig. 8). Variation in coloration and pattern is extensive due to this species' having very different dark and light phases and its ability to substrate-match (see Grismer 2011a). Color pattern variation in the paratypes described here is based on preserved material. LSUHC 9059, 9447, and 11418 have more boldly marked dorsal bands. Dorsal caudal bands in LSUHC 11418 are much more prominent than those of the holotype. Dark, subcaudal banding in LSUHC 9447 and 11418 is far more distinct than that of the holotype and in LSUHC 9059 and 10991 the

TABLE 6. Meristic, mensural (in mm), and diagnostic characters of *Ptychozoon cicakterbang* **sp. nov**. Gn = Gunung (mountain) and P = Pulau (island). See Materials and methods for character abbreviations. Numbers in parentheses refer to numbered localities in Figure 1. / = data unobtainable; r = tail partially or completely regenerated.

	LSUHC 10648 (12) Gn. Jerai holotype	LSUHC 5783 (2) P. Sibu paratype	LSUHC 5597 (2) P. Sibu paratype	LSUHC 9059 (8) P. Perhentian Besar paratype	LSUHC 9447 (13) P. Langkawi paratype	LSUHC 8709 (8) P. Perhentian Besar paratype	LSUHC 11418 (6) P. Bidong paratype	LSUHC 11058 (11) Gn. Stong paratype	LSUHC 10978 (5) Lata Belatan paratype
sex	f	m	m	f	f	m	m	f	f
supralabials to middle of eyeball (SU)	10	11	10	11	9	11	11	10	11
infralabials (IL)	14	15	14	15	12	13	14	13	12
supra-auricular lobe	yes	yes	yes	yes	yes	yes	yes	yes	yes
midbody dorsal scales (MB)	86	84	85	98	91	100	95	86	79
midbody ventral scales (VS)	42	36	34	44	32	32	44	36	30
enlarged pore-bearing precloacal scales in males (PP)	/	17	21	/	/	21	25	/	/
enlarged precloacal scales (PS)	23	18	23	25	22	23	26	24	20
enlarged post-precloacal scale rows (PPS)	5	5	5	7	6	6	7	8	5
transversely expanded 4th toe lamellae (TL4)	17	16	17	16	17	16	16	15	16
enlarged dorsal caudal scales forming whorls	yes	yes	yes	yes	yes	yes	yes	yes	yes
scales across widest portion of caudal flap (CF)	34	28	26	28	30	25	29	/	27
edges of caudal flap smooth or crenulated	crenulated	crenulated	crenulated	crenulated	crenulated	crenulated	crenulated	crenulated	crenulated
thick postorbital stripe	no	no	no	no	no	no	no	no	no
irregularly shaped, white vertebral markings	absent	absent	absent	absent	absent	absent	absent	absent	absent
SVL	86.0	81.9	74.7	84.6	82.0	80.1	84.2	93.4	91.3
TL	76.4	69.8r	77.2	88.3	86.7	80.5	79.1	65.6r	81.5
TW	7.9	6.7	6.3	7.2	7.1	7.0	7.3	6.8	7.4
HL	23.5	22.7	21.9	24	24.0	22.7	22.5	25	23.2
HW	17.8	16.7	15.8	17.1	17.4	16.7	17,4	19.4	16.3
HD	9.3	8.9	8.8	9.2	8.7	9.7	9.1	10.3	9.2
SNL	10.6	10.6	10.2	11.1	10.4	10.1	9.7	11.5	10.7
ED	5.2	4.7	4.5	3.7	4.5	5.6	5.6	6.7	6.0
TD	2.7	1.6	1.3	2.0	2.1	1.5	2.2	2.2	2.8
IN	3.4	2.6	2.7	2.9	2.4	2.8	3.0	3.4	3.1
IO	2.2	2.9	2.9	2.1	2.2	2.1	2.3	3.5	2.3
AXG	39.7	41.2	40.5	43.9	42.7	38	40.1	44.4	45.4
FL	9.6	10.6	9.5	9.9	10.6	8.8	10.0	11.4	11.0
TBL	13.2	14.6	13.8	13.7	14.6	12.9	13.7	14.1	16.0

TABLE 6. (Continued)

	LSUHC 11439 P. Bidong (6) non-type	LSUHC 9891 Lata Tembaka (10) non-type	LSUHC 11234 Lata Belatan (5) non-type	LSUHC 11236 Lata Belatan (5) non-type	LSUHC 11235 Lata Belatan (5) non-type	LSUHC 5539 P. Sibu (2) non-type	LSUHC 9409 P. Redang (7) non-type	LSUHC 6437 P. Tioman (3) non-type
sex	f	f	f	f	f	f	f	f
supralabials to middle of eyeball (SU)	9	10	10	9	9	12	13	10
infralabials (IL)	13	12	11	11	12	12	14	12
supra-auricular lobe	yes	yes	yes	yes	yes	yes	yes	yes
midbody transverse dorsal scales (MB)	94	80	91	105	95	81	96	84
midbody transvers ventral scales (VS)	48	43	34	39	39	38	35	39
enlarged pore-bearing precloacal scales in males (PP)	/	/	/	/	/	/	/	/
enlarged precloacal scales (PS)	28	22	26	24	20	18	22	23
enlarged post-precloacal scale rows (PPS)	8	5	6	6	6	6	5	6
transversely expanded 4th toe lamellae (TL4)	17	17	15	17	16	16	16	14
enlarged dorsal caudal scales forming whorls	yes	/	/	yes	/	yes	yes	yes
scales across widest portion of caudal flap (CF)	33	/	/	33	/	25	29	26
edges of caudal flap smooth or crenulated	crenulated	crenulated	crenulated	crenulated	crenulated	crenulated	crenulated	crenulated
thick postorbital stripe	absent	absent	absent	absent	absent	absent	absent	absent
irregularly shaped, white vertebral markings	no	no	no	no	no	no	no	no
SVL	92.6	90.0	89.4	86.5	87.9	85.3	87.4	70.6
TL	80.2	76.1R	58.6	76.8	/	82.8	86.8	71.3
TW	8.3	7.3	7.3	7.3	7.3	6.8	6.8	5.3
HL	26.1	25.5	23.6	21.2	23.8	23.5	23.7	19.9
HW	20.3	18.6	17.2	15.7	18	17	17.7	14.3
HD	9.8	9.7	9.0	8.7	9.5	8.3	8.8	6.8
SNL	11.7	11.9	10.9	10.2	10.9	11.3	11.1	9.1
ED	6.5	6.3	5.5	5.4	5.5	4.1	4.2	4.2
TD	2.0	2.4	2.1	2.3	2.5	1.7	1.7	1.2
IN	3.0	3.2	3.0	3.1	3.1	3.2	3.1	2.6
IO	2.9	3.4	2.8	1.6	2.3	3.1	3.2	2.6
AXG	43.2	43.3	43.8	41.5	41.8	43.4	42.0	34.5
FL	11.4	9.5	9.7	9.7	8.9	9.4	9.7	8.5
TBL	14.8	14.6	13.1	13.2	12.4	14.0	17.0	12.6

banding is more defined than that of the holotype but not nearly as much as the former three specimens. The belly of LSUHC 11418 is much more densely stippled than other specimens of the type series. The parachute scales of the body patagia do not imbricate in LSUHC 5539, 5597, 6437, 8709, and 9059 whereas in the holotype and the other paratypes they are subimbricate. The tails of LSUHC 5783 and 11058 are regenerated and bear no caudal lobes. Males LSUHC 5597, 5783, 8709, and 11418 have 17–25 enlarged pore-bearing precloacal scales. Meristic differences amongst the type material and the additional specimens examined are presented in Table 6.

Comparisons (Tables 4, 5; Figs. 3, 5, 6). *Ptychozoon cicakterbang* **sp. nov.** differs from all other species of *Ptychozoon* in having a prominent supra-auricular lobe as opposed to a small ridge or no enlargement at all. It differs further from *P. intermedium* Taylor, 1915*, P. kuhli* (Stejneger, 1902)*,* and *P. trinotaterra* in lacking as opposed to having caudal tubercles. From *P. intermedium, P. rhacophorus* (Boulenger, 1899)*, P. trinotaterra,* and *P. kaengkrachanense* it differs in having four body bands as opposed to 0–3. *Ptychozoon cicakterbang* **sp. nov.** differs from *P. bannaense* Wang, Wang, & Liu, 2016*, P. horsfieldii, P. intermedium, P. kuhli, P. nicobarense, P. rhacophorus, P. trinotaterra,* and *P. kaengkrachanense* in having an emargination between the pre-antebrachial flap and digit I as opposed to no emargination. From *P. popaense* it differs by having a maximum SVL of 93.4 mm versus 86.2 mm, 14–17 subdigital lamellae on the fourth toe versus 13 or 14, the absence versus the presence of a thick, dark postorbital stripe; and the absence versus the presence of large, irregularly shaped, white, vertebral markings. *Ptychozoon cicakterbang* **sp. nov.** differs futher from *P. lionotum, P. kabkaebin* **sp. nov.**, and *P. tokehos* **sp. nov.** by having a significantly higher mean number of infralabials and a prominent supra-auricular lobe versus a slightly raised ridge. From *C. tokehos* **sp. nov.** it differs further by having a significantly higher mean number of subdigital lamellae on the fourth toe, a higher mean number of ventral scales, and a significantly longer axilla-groin length. From *P. lionotum* it differs even further by having, as opposed to lacking, prominent ridges on the ventral surface of the patagia and weakly crenulated as opposed to smooth caudal flap edges. From *C. kabkaebin* **sp. nov.** and *P. lionotum* it differs further by having a significantly higher mean number of supralabial scales and midbody scales and caudal whorls composed of enlarged scales. From *C. kabkaebin* **sp. nov.** it differs further by lacking, as opposed to having, a thick, dark, postorbital stripe. From *C. lionotum* it differs further by having a significantly narrower head. *Ptychozoon cicakterbang* **sp. nov.** is well-separated from other species previously recognized as *P. lionotum* in the PCA and DAPC and occupies a significantly different position along PC1 from that of *P. kabkaebin* **sp. nov.** and *P. tokehos* **sp. nov.** and along PC2, it occupies a significantly different positon from that of *P. lionotum.* From these three species, it is further separated by an uncorrected pairwise sequence divergence of 4.1–14.4%. Combinations of other characters differentiating *P. cicakterbang* **sp. nov.** from other more distantly related species are presented in Table 5.

Distribution (Fig. 1). *Ptychozoon cicakterbang* **sp. nov.** ranges throughout Peninsular Malaysia and its associated east and west coast islands and most probably extends into extreme southern Thailand. A population has also been reported from Natuna Besar Island, Indonesia that lies between Peninsular Malaysia and Borneo (Leong *et al.* 2003).

Etymology. The specific epithet *cicakterbang* is derived from the Malay word for flying lizards. The word "cicak" means lizard and "terbang" means flight. The term is used for both *Ptychozoon* and *Draco.*

Natural history. *Ptychozoon cicakterbang* **sp. nov.** is found on trees of varying sizes in primary and old secondary, lowland dipterocarp forests (Fig. 9) up to approximately 800 meters in elevation (Dring 1979; Grismer 2011a,b; Grismer *et al.* 2011). On Pulau Sibu, it occurs at sea level on small trees within coastal forest adjacent to mangrove swamps (Grismer 2011a) and can often be found sleeping on the smaller branches of small trees and large shrubs during the day and night less than two meters above the ground (Grismer 2011a; Grismer *et al.* 2011). When alarmed, it may jump to the ground to escape. On Pulau Lang Tengah, Terengganu, specimens were observed on the ground eating winged termites on a rainy evening during a storm (Evan S. H. Quah; pers. obs.). *Ptychozoon cicakterbang* **sp. nov.** is adept at substrate matching and can vary considerably in coloration and pattern from one area to the next (Fig. 8).

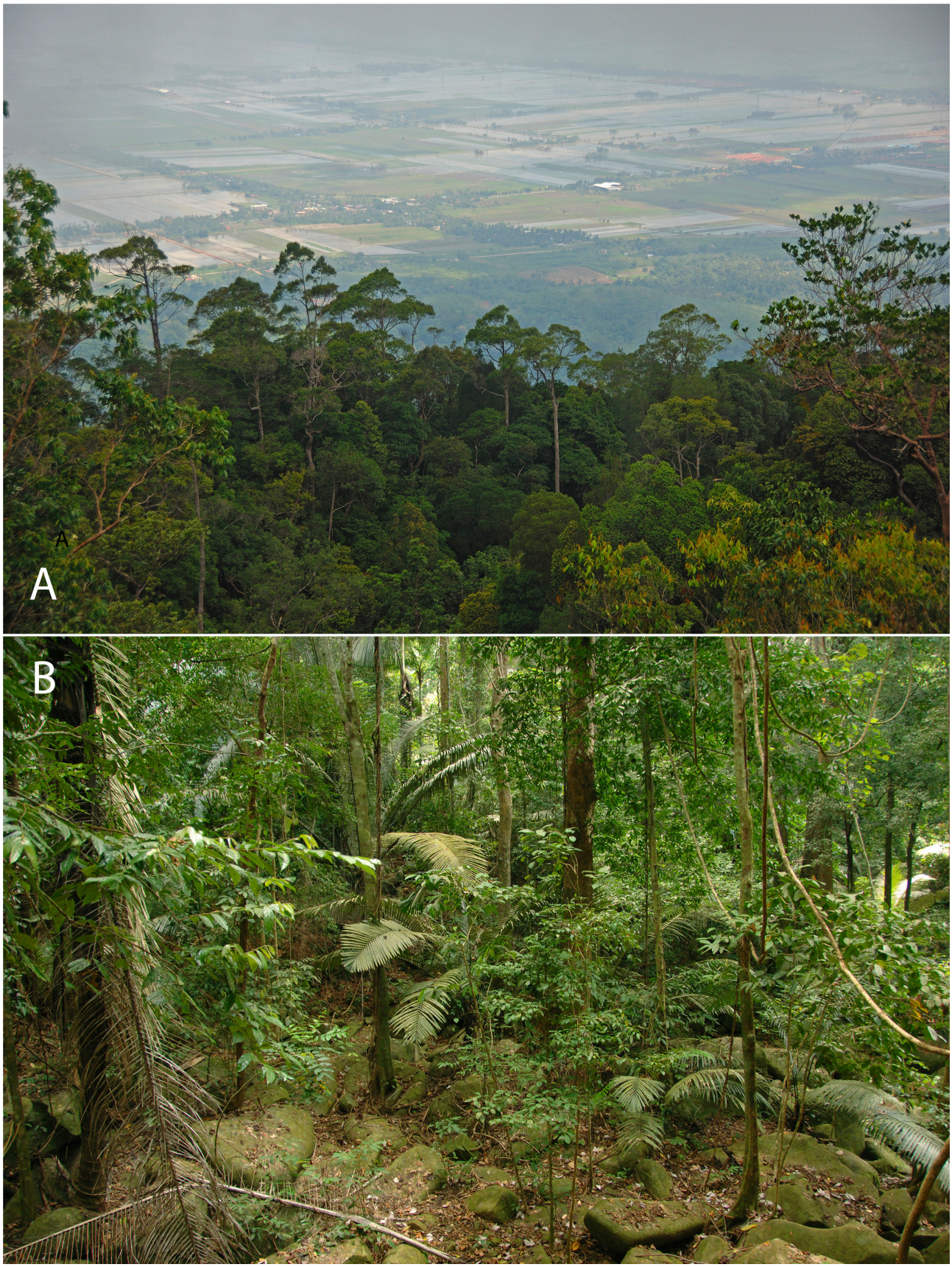

FIGURE 9. Habitat of *Ptychozoon cicakterbang* **sp. nov.** A. Forest at the type locality of Gunung Jerai, Kedah, Peninsular Malaysia. B. Microhabitat along the Tekek-Juara Trail, Pulau Tioman, Peninsular Malaysia.

***Ptychozoon kabkaebin* sp. nov.**
Lao Parachute Gecko
Fig. 10

Ptychozoon lionotum Teynié *et al.,* 2014:35 (in part); Manthey & Manthey, 2017:42

Holotype. NCSM 80585 adult female collected by Sengvilay Seateun and Misan Keooudone on 16 June 2012 from Houay Ta Ang Stream, Pakkading District, Bolikhamxay Province, Laos (18.32997°N, 103.99140°E, 163 m above sea level).

Paratypes. FMNH 271140 adult female collected by Bryan L. Stuart, Somphouthone Phimmachak, and Niane Sivongxay on 28 May 2007 from Nakai-Nam Theun National Protected Area, Phou Ack Mountain, Boualapha District, Khammouan Province, Laos (17.64433°N, 105.73667°E, 980 m above sea level); and NUOL 00036 adult female collected by Bryan L. Stuart, Somphouthone Phimmachak, and Jennifer A. Sheridan on 17 May 2013 from Nakai-Nam Theun National Protected Area, Phou Ack Mountain, Boualapha District, Khammouan Province, Laos (17.64256 °N, 105.73608 °E, 992 m above sea level).

Diagnosis. *Ptychozoon kabkaebin* **sp. nov.** differs from all other species of *Ptychozoon* by having the following unique combination of characters: a maximum SVL of 95.4 mm; supranasals not in contact; 8–10 supralabials; 10–12 infralabials; infra-auricular cutaneous flap; weak, supra-auricular ridge present; no dorsal or caudal tubercles; imbricate parachute support scales on dorsal surface of patagia; no prominently raised ridges on ventral surface of patagia; 78–82 midbody dorsal scales; 33–38 ventral scales; an emargination between the pre-antebrachial flap and digit I; no enlarged femoral scales; 22 or 23 enlarged precloacal scales; 5–7 rows of enlarged post-precloacal scales; 13–17 transverse subdigital lamellae on fourth toe; no enlarged dorsal caudal scales forming whorls; approximately 27–30 scales across widest portion of caudal flap; distal lobes fusing to form a short, narrow caudal flap; edges of caudal flap weakly crenulated; caudal lobes angled posteriorly; caudal lobes decrease posteriorly in size; thick, dark, postorbital stripe; four dark body bands between limb insertions; irregularly shaped, white, vertebral markings variably present; and subcaudal region banded in adults (Tables 4, 5).

Description of holotype. Adult female SVL 85.1 mm; head moderate (HL/SVL 0.27), wide (HW/HL 0.79), depressed (HD/HL 0.41), distinct from neck; snout rounded at tip in dorsal profile; prefrontal region weakly concave; lores rounded; rostral scale large, rectangular, in contact posteriorly with two supranasals and two small postnasals, dorsolaterally with nostrils, and laterally with first supralabials; supralabials (10R,L) to mid-orbital position; infralabials (12R,L); nostrils elliptical with long axes oriented obliquely, occupying anterior portion of nasal scale, bordered anteriorly by rostral, dorsally by supranasal, posteriorly by six postnasals of varying sizes (upper largest), and ventrally by first supralabial; scales on rostrum granular slightly larger than granular scales on top of head and occiput; eyes large (ED/HL 0.21), less than snout length; pupil vertically elliptical, crenelated; supraciliaries elongate, posteriormost weakly pointed; auricular opening rounded, bearing a weak, supra-auricular ridge; tympanum deeply sunk; infra-auricular flap broad, rounded, extending from below corner of mouth to lateral margin of neck midway between posterior margin of ear opening and forelimb insertion, measuring 5.6 mm at its widest point; dorsal scales of infra-auricular flap large, subimbricate proximally, small juxtaposed distally, ventral flap scales minute and granular; mental triangular, as wide as deep, bordered laterally by first infralabials and posteriorly by paired, rectangular postmentals contacting medially for 100% of their length; one row of enlarged sublabials bordering infralabials, anteriormost largest; gular scales small, rounded, grading into larger imbricating throat and subimbricate pectoral and ventral scales.

Body dorsoventrally depressed, relatively stout (AXG/SVL 0.47); patagia 7.4 mm at midpoint of body bearing enlarged, subimbricate, rectangular scales dorsally, minute, juxtaposed, subrectangular scales ventrally; ventral surface not bearing raised ridges of granular scales; 81 minute, flat, round, juxtaposed midbody dorsal scales, largest mid-dorsally; no large flat dorsal scales immediately anterior to the hind limb insertions; 35 transverse rows of large, smooth, flat, subimbricate ventral scales much larger than dorsal scales, decreasing in size laterally into granular scales at the base of the flap; 22 enlarged, precloacal scales; seven rows of enlarged, post-precloacal scales; and scales immediately anterior to vent granular.

Limbs short, robust (FL/SVL 0.12; TBL/SVL 0.16); dorsal scales of forelimbs, flat, juxtaposed, larger than dorsal body scales; ventral forelimb scales subimbricate; anterior and posterior margins of forelimbs, and posterior margins of hind limbs bearing wide, cutaneous flaps; that of anterior margin of forearm (*i.e.* pre-antebrachial flap) emarginated distally and terminates low on the base of digit I, that of the foreleg does not reach the base of digit I;

scales of forelimb flaps large, elongate, subimbricate; those of hind limb flaps much smaller, rounded, subimbricate; palmar scales smooth, rounded; digits fully webbed, relatively short, dorsoventrally compressed; undivided transverse subdigital lamellae number 15 (I), 14 (II), 13 (III), 15 (IV), 14 (V), distalmost lamellae V-shaped; claws arise from within the dorsal surface of digital pads; claw of digit I replaced by an enlarged, flat scale; dorsal scales of hind limbs, flat, juxtaposed, larger than dorsal body scales; ventral scales of hind limbs flat, subimbricate, smaller than ventral scales of belly; flat; scales of anterior margin of thigh subimbricate; plantar scales smooth, subimbricate; digits fully webbed; transverse subdigital lamellae number 10 (I), 13 (II), 13 (III), 14 (IV), 11 (V), distalmost lamellae V-shaped; claws arise from within the dorsal surface of digital pads, and claw of digit I replaced by an enlarged, flat scale.

Tail original, flattened, same length as SVL (TaL/SVL 1.00); two median rows of transversely widened, smooth subcaudals anteriorly becoming less regular and broken up posteriorly; postcloacal scales large, flat, imbricate; dorsal caudals flat, juxtaposed, larger than dorsal body scales and not bearing transversely aligned whorls of enlarged scales; tail width and caudal lobes decrease posteriorly; 23 caudal lobes on each side slightly angled posteriorly; and tail terminates in a short flap (11.9 mm) bearing weakly crenulated edges.

TABLE 7. Meristic, mensural (in mm), and diagnostic characters of *Ptychozoon kabkaebin* **sp. nov.** See Materials and methods for character abbreviations. / = data unobtainable. Numbers in parentheses refer to numbered localities in Figure

	NCSM 80585 (33) Pakkading, Laos holotype	NUOL 00036 (32) Phou Ack, Laos paratype	FMNH 271140 (31) Phou Ack, Laos paratype
sex	f	f	f
supralabials to middle of eyeball (SU)	10	8	8
infralabials (IL)	12	10	10
supra-auricular lobe	small ridge	small ridge	small ridge
midbody dorsal scales (MB)	81	82	78
midbody ventral scales (VS)	35	38	33
enlarged pore-bearing precloacals in males (PP)	/	/	/
enlarged precloacal scales (PS)	/	/	/
enlarged post-precloacal scale rows (PPS)	7	6	5
transversely expanded 4th toe lamellae (TL4)	14	17	13
enlarged dorsal caudal scales forming whorls	absent	absent	absent
scales across widest portion of caudal flap (CF)	28	30	27
edges of caudal flap smooth or crenulated	weakly crenulated	weakly crenulated	weakly crenulated
thick postorbital stripe	yes	yes	yes
irregularly shaped, white vertebral markings	no	no	yes
SVL	85.1	89.1	95.4
TL	85.2	83.1	94.8
TW	7.5	8.5	9.4
HL	22.7	23.5	25.6
HW	18.0	17.6	18.8
HD	9.4	9.5	10.4
SNL	9.7	9.7	10.5
ED	4.7	4.9	5.2
TD	2.2	3.3	2.2
IN	2.9	3.3	3.3
IO	1.8	2.6	1.9
AXG	39.8	39.1	45.1
FL	10.0	10.5	10.6
TBL	13.7	14.1	15.9

FIGURE 10. *Ptychozoon kabkaebin* **sp. nov.** A. Paratype NUOL 00036 from Nakai-Nam Theun National Protected Area, Phou Ack Mountain, Boualapha District, Khammouan Province, Laos. Photograph by B. L. Stuart. B. Paratype FMNH 271140 from Nakai-Nam Theun National Protected Area, Phou Ak Mountain, Boualapha District, Khammouan Province, Laos. Photograph by B. L. Stuart. C. Holotype NCSM 80585 from Houay Ta Ang Stream, Pakkading District, Bolikhamxay Province, Laos. Photograph by L. L. Grismer.

FIGURE 11. Habitat of *Ptychozoon kabkaebin* **sp, nov.** at Nakai-Nam Theun National Protected Area, Phou Ack Mountain, Boualapha District, Khammouan Province, Laos. Photograph by B. L. Stuart.

Light phase coloration and pattern in preservative (Fig. 10). Dorsal ground color of head, body, and tail light-brown; top of head essentially unicolor; labial scales much lighter than body, demarkated by thin, dark lines at their junctures; infra-auricular flap same lighter color as labial scales and gular region; four, thin, sinuous dorsal bands between limb insertion eventually transitioning into approximately two dark-brown caudal bands towards the end of the tail; terminus of caudal flap white; subcaudal region mottled anteriorly and banded; pectoral region, belly, and ventral surfaces of limbs dull-white with no stippling.

Variation. Variation in coloration and pattern varies due to this species' having dark and light phases and its ability to substrate match. Color pattern variation in the paratypes described here is based on preserved material. The paratypes closely approximate the holotype in coloration and pattern. Caudal banding is distinct in all specimens. The wide white band on the caudal flap extends all the way to the tip in the holotype whereas in the paratypes a black band encompasses the tip. Paratype FMNH 271140 has irregularly shaped, white vertebral markings that are absent in the paratype NUOL 00036 and the holotype. Variation in meristic characters is presented in Table 7.

Comparisons (Tables 4, 5; Figs. 3, 5, 6). Differences between *Ptychozoon kabkaebin* **sp. nov.** and *P. cicakterbang* **sp. nov.** are listed above in the comparisons section of *P. cicakterbang* **sp. nov.** *Ptychozoon kabkaebin* **sp. nov.** differs from *P. intermedium, P. kuhli,* and *P. trinotaterra* in lacking, as opposed to having, caudal tubercles. From *P. intermedium, P. nicobarense, P. rhacophorus, P. trinotaterra,* and *P. kaengkrachanense* it differs in having four body bands as opposed to 0–3. *Ptychozoon kabkaebin* **sp. nov.** differs from *P. bannaense, P. horsfieldii, P. intermedium, P. kuhli, P. nicobarense, P. rhacophorus, P. trinotaterra,* and *P. kaengkrachanense* in having an emarginated pre-antebrachial flap as opposed to lacking an emargination. From *P. popaense* it differs by having a maximum SVL of 95.4 mm versus 86.2 mm. *Ptychozoon kabkaebin* **sp. nov.** differs from *P. lionotum,* and *P. tokehos* **sp. nov.** by having a significantly higher mean number of infralabials. *Ptychozoon kabkaebin* **sp. nov.** differs from *P. tokehos* **sp.**

nov. in having a significantly wider head. Even though *Ptychozoon kabkaebin* **sp. nov.** and *P. tokehos* **sp. nov.** have nearly discrete differences in their numbers of midbody scales (78–82 and 80–95, respectively), their mean differences (80.3 versus 89.0) were not significantly different in the ANOVA (p=0.09) although they were significantly different in a two-sample Student t-test (t=5.585; p=0.002). *Ptychozoon kabkaebin* **sp. nov.** is the sister species of *P. lionotum* but differs further from it by having a significantly shorter snout. *Ptychozoon kabkaebin* **sp. nov.** is well-separated from *P. cicakterbang* **sp. nov.** and *P. lionotum* in the PCA and from all species in the DAPC where their 95% confidence ellipses do not overlap. *Ptychozoon kabkaebin* **sp. nov.** occupies a significantly different position along PC1 from that of *P. cicakterbang* **sp. nov.** and along PC2, it occupies a significantly different positon from that of *P. tokehos* **sp. nov.** From all species of the *lionotum* group it differs by having an uncorrected pairwise sequence divergence of 4.1–14.4%. Combinations of other characters differentiating *P. kabkaebin* **sp. nov.** from the other more distantly related species are presented in Table 5.

Distribution (Fig. 1). *Ptychozoon kabkaebin* **sp. nov.** is endemic to the eastern parts of northern and central Laos although it will likely be found in adjacent areas of central Vietnam.

Etymology. The specific epithet *kabkaebin* is the Lao word used for *Ptychozoon.*

Natural history. NCSM 80585 was collected during the day from beneath a house on stilts that was located along a stream in degraded semi-evergreen forest at 160 m in elevation. FMNH 271140 was collected during the day (1115 h) at 980 m in elevation and NUOL 00036 was collected during the night (2130 h) at 992 m in elevation, both on large boulders in a mosaic of evergreen, deciduous, and pine forest with grassy understory at the edge of a high cliff on a steep escarpment. (Fig. 11).

Ptychozoon tokehos sp. nov.
Cambodian Parachute Gecko
Fig. 12

Ptychozoon kuhli Smith, 1935:119 (in part)
Ptychozoon lionotum Bourret 1937–1947 in Bourret, 2009:169 (in part); Smith, 1935:118 (in part); Manthey & Grossmann, 1997:247 (in part); Cox *et al.,* 1998:81 (in part); Das, Dattagupta, & Gayen, 1998:131 (in part); Chan-ard *et al.,* 1999:132 (in part); Pauwels *et al*., 2000: 132; Kluge, 2001:25 (in part); Pauwels *et al*., 2002: 27; Stuart & Emmet, 2006:18; Grismer *et al.,* 2008:22; Nguyen *et al.,* 2009:236; Grismer, 2011a:532, 2011b:139; Grismer *et al.,* 2011:62 (in part); Sumontha *et al*., 2012: 74; Herr & Lee, 2016:111; Vassilieva *et al.,* 2016:162; Grismer & Quah, 2019:234.
Ptychozoon lionatum [sic.] Taylor, 1963:807; Grismer *et al.,* 2007:231 (in part)
Ptychozoon trinotaterra Grismer *et al.,* 2011:64

Holotype. FMNH 261853 adult female, collected by Bryan L. Stuart and Dara Anon 5 June 2000 from Kirirom National Park, Phnom Sruoch District, Kampong Speu Province, Cambodia (11.32611°N, 104.06556°E, 700 m in elevation).

Paratypes. FMNH 261851–52 bear the same collection data as the holotype except they were collected on 3 June 2000. FMNH 261854 bears the same collection data as the holotype except it was collected on 5 November 2000 by Joe Walston. CBC 03162 adult female collected by Neang Thy on 9 June 2017 from Bokor National Park, Teuk Chou District, Kampot Province, Cambodia (10.60156°N, 104.03200°E, 325 m in elevation). NCSM 98986 adult female collected by Neang Thy on 10 June 2017 from Bokor National Park, Teuk Chou District, Kampot Province, Cambodia (10.60372°N, 104.02944°E, 328 m in elevation). NCSM 98987 adult female collected by Neang Thy on 12 June 2017 from Bokor National Park, Teuk Chou District, Kampot Province, Cambodia (10.58753°N, 104.03269°E, 315 m in elevation). FMNH 177359 adult male collected by Edward H. Taylor on 11 June 1969 from the Khao Chong Reserve, Trang Province, Thailand (7.54350°N 99.79800°E, 127 m in elevation). FMNH 181844 adult male collected by W. Ronald Heyer on 11 June 1969 from Pak Thong Chai District, Nakhon Ratchasima Province, Sakaerat (Environmental Research Station), Thailand (14.50000°N, 100.86670°E, 16 m in elevation).

Additional specimens examined. FMNH 177358 and 177550 adult females collected by Edward H. Taylor on 11 June 1969 from the Khao Chong Reserve, Trang Province, Thailand (7.54350°N 99.79800°E, 127 m in elevation). FMNH 181823–24, 181828–29 adult males collected by W. Ronald Heyer on 11 June 1969 from Pak Thong Chai District, Nakhon Ratchasima Province, Sakaerat (Environmental Research Station), Thailand (14.50000°N, 100.86670°E, 16 m in elevation). USNM 587523 adult female collected by Daniel Mulcahy on 27 May 2015 from the proposed Lenya National Park, Tanintharyi Region, Myanmar (11.05080°N 98.91720°E, 58 m in elevation).

FMNH 177548 adult male collected by Oliver G. Young in 1961 from Chiang Mai, Chiang Mai District, Chiang Mai Province, Thailand (18.79528°N 98.99861°E, 314 m in elevation). MNHN 1998.590 and 1999.7661 collected on 16 February 1998 by Olivier S. G. Pauwels from the Phang-Nga Wildlife Breeding Station, Muang District, Phang Nga Province, Thailand (8.45014°N, 98.525532°E, 154 m in elevation).

Diagnosis. *Ptychozoon tokehos* **sp. nov.** differs from all other species of *Ptychozoon* by having the following unique combination of characters: a maximum SVL of 97.5 mm; supranasals not in contact; 8–11 supralabials; 10–12 infralabials; infra-auricular cutaneous flap; weak supra-auricular ridge present; no dorsal or caudal tubercles; imbricate parachute support scales on dorsal surface of patagia; prominently raised ridges on ventral surface of patagia; 80–95 midbody dorsal scales; 30–37 ventral scales; an emargination between the pre-antebrachial flap and digit I; no enlarged femoral scales; 20–24 pore-bearing precloacal scales in males; 18–25 enlarged precloacal scales; 4–7 rows of enlarged post-precloacal scales; 13–18 transverse subdigital lamellae on the fourth toe; approximately 28–34 scales across the widest portion of the caudal flap; enlarged dorsal caudal scales forming intermittent whorls; distal lobes fusing to form a short, narrow, caudal flap; edges of caudal flap smooth; caudal lobes angled posteriorly; caudal lobes variably showing posterior reduction in size; postorbital striping variable; four dark body bands between limb insertions; and irregularly shaped, white, vertebral markings usually not present (absent in 14 of 16 specimens; Tables 4, 5).

Description of holotype. Adult female SVL 97.5 mm; head moderate (HL/SVL 0.25), wide (HW/HL 0.79), depressed (HD/HL 0.44), distinct from neck; snout rounded at tip in dorsal profile; prefrontal region weakly concave; lores rounded; rostral scale large, rectangular, in contact posteriorly with two supranasals and one postnasal, dorsolaterally with nostrils, and laterally with first supralabials; supralabials (10R, 9L) to mid-orbital position; infralabials (12R, 11L); nostrils elliptical with long axes oriented obliquely, occupying anterior portion of nasal scale, bordered anteriorly by rostral, dorsally by supranasal, posteriorly by four postnasals of varying sizes (upper largest), and ventrally by first supralabial; scales on rostrum granular larger than granular scales on top of head and occiput; eyes large (ED/HL 0.23), less than snout length; pupil vertically elliptical, crenelated; supraciliaries elongate, posteriormost pointed; auricular opening rounded, bearing a weak supra-auricular ridge; tympanum deeply sunk; infra-auricular flap broad, rounded, extending from below corner of mouth to lateral margin of neck midway between posterior margin of ear opening and forelimb insertion, measuring 5.0 mm at its widest point; dorsal scales of infra-auricular flap large, subimbricate proximally, small juxtaposed distally, ventral scales of flap minute and granular; mental triangular, as wide as deep, bordered laterally by first infralabials and posteriorly by paired, rectangular postmentals, posterior section of left postmental divided into three smaller scales; one row of enlarged sublabials bordering infralabials, anteriormost largest; gular scales granular, grading into larger imbricating throat and subimbricate pectoral and ventral scales.

Body dorsoventrally depressed, relatively stout (AXG/SVL 0.53); patagia 8.9 mm at midpoint of body bearing enlarged, subimbricate, rectangular scales dorsally, minute, juxtaposed, subrectangular scales ventrally, ventral surface bearing raised scaly ridges extending from body to edge of flap; 88 minute, flat, round, juxtaposed midbody dorsal scales, largest mid-dorsally; no large, flat, dorsal scales immediately anterior to the hind limb insertions; 36 transverse rows of large, smooth, flat, subimbricate ventral scales much larger than dorsal scales, decreasing in size laterally into granular scales at the base of the flap; 21 enlarged, precloacal scales; five rows of enlarged, post-precloacal scales; and scales immediately anterior to vent granular.

Limbs short, robust (FL/SVL 0.10; TBL/SVL 0.17); dorsal scales of forelimbs, flat, juxtaposed, larger than dorsal body scales; ventral forelimb scales small, subimbricate; anterior and posterior margins of forelimbs, and posterior margins of hind limbs bearing wide, cutaneous flaps; that of anterior margin of forearm (*i.e.* pre-antebrachial flap) emarginated distally and terminates low on the base of digit I, that of the foreleg does not reach the base of digit I; scales of forelimb flaps large, elongate, subimbricate; those of hind limb flaps smaller, more rounded, subimbricate; palmar scales smooth, rounded; digits fully webbed, relatively short, dorsoventrally compressed; undivided transverse subdigital lamellae number 11 (I), 13 (II), 12 (III), 13 (IV), 12 (V), distalmost lamellae V-shaped; claws arise from within the dorsal surface of digital pads; claw of digit I replaced by an enlarged, flat scale; dorsal scales of hind limbs, flat, juxtaposed, same size as dorsal body scales; ventral scales of hind limbs flat, subimbricate, smaller than ventral scales of belly; scales of anterior margin of thigh large, subimbricate; plantar scales smooth, subimbricate; digits fully webbed; transverse subdigital lamellae number 11 (I), 12 (II), 14 (III), 15 (IV), 13 (V), distalmost lamellae V-shaped; claws arise from within the dorsal surface of digital pads, and claw of digit I replaced by an enlarged, flat scale.

TABLE 8. Meristic, mensural (in mm), and diagnostic characters of *Ptychozoon tokehos* **sp. nov.** P = Phnom (mountain). See Materials and methods for character abbreviations. / = data unobtainable. r = tail partially or completely regenerated. Numbers in parentheses refer to numbered localities in Figure 1.

	FMNH 261853 (25) Kirirom Cambodia holotype	FMNH 261851 (25) Kirirom Cambodia paratype	FMNH 261852 (26) Kirirom Cambodia paratype	FMNH 261854 (26) Kirirom Cambodia paratype	NCSM 98986 (27) Bokor Cambodia paratype	CBC 03162 (27) Bokor Cambodia paratype	NCSM 98987 (27) Bokor Cambodia paratype	FMNH 177359 (15) Khao Chong Thailand paratype	FMNH 18144 (21) Sakaerat Thailand paratype
sex	f	m	f	f	f	f	f	m	m
supralabials (SU)	10	10	10	8	8	10	8	11	9
infralabials (IL)	11	10	11	10	11	11	10	12	11
supra-auricular lobe	small ridge	small ridge	small ridge	small ridge	small ridge	small ridge	small ridge	small ridge	small ridge
midbody transverse dorsals (MB)	88	92	84	83	88	90	87	86	94
midbody transverse ventral scales (VS)	36	36	35	36	34	33	34	30	35
enlarged pore-bearing precloacal scales in males (PP)	/	21	/	/	/	/	/	23	22
enlarged precloacal scales (PS)	21	24	20	20	22	22	25	25	22
enlarged post-precloacal scale rows (PPS)	5	5	6	5	7	6	5	4	5
transversely expanded 4th toe lamellae (TL4)	15	18	13	13	15	15	15	15	17
scales across widest portion of caudal flap (CF)	34	32	/	/	34	28	29	34	34
edges of flap smooth or crenulated	smooth	smooth	/	/	smooth	smooth	smooth	/	/
thick postorbital marking	yes	yes	faint	faint	no	no	no	no	no
irregularly shaped, white vertebral markings	yes	no	yes	/	no	no	no	no	no
SVL	97.5	82.0	75.6	89.3	83.8	87.2	84.4	78.5	85.6
TL	86.1	97.5	58.6r	45.8r	broken	83.3	75.0	75.0	81.5
TW	7.8	9.6	6.4	7.4	7.3	7.9	6.8	7.0	8.2
HL	24.7	23.6	21.7	24.4	22.4	23.8	22.8	21.7	23.8
HW	19.5	18.6	16.3	18.2	16.5	17.2	16.7	16.0	17.8
HD	10.8	9.9	8.4	11.2	8.8	9.4	9.4	8.7	9.3
SNL	12.0	11.6	9.5	10.7	9.9	9.4	9.4	8.7	10.9
ED	5.7	3.2	4.4	5.1	5.2	5.5	5.0	9.7	5.4
TD	3.3	1.0	2.7	3.1	2.1	2.2	2.2	1.9	2.0
IN	3.9	3.4	2.8	3.5	3.2	3.3	3.3	1.8	3.2
IO	9.7	2.5	7.9	9.1	1.9	2.2	2.2	7.9	3.5
AXG	51.8	44.2	34.3	39.6	41.0	45.0	40.0	36.1	38.1
FL	9.9	19.3	9.5	10.1	9.5	10.1	9.5	10.0	8.9
TBL	16.7	16.6	13.1	14.6	13.3	13.3	12.2	12.3	12.3

TABLE 8. Continued.

	MNHN 1990.0590 (16)	MNHN 1999.7661 (16)	FMNH 177358 (15)	FMNH 177550 (15)	FMNH 181823 (21)	FMNH 181824 (21)	FMNH 181828 (21)	FMNH 181829 (21)	FMNH 177548 (20)	USNM 587523 (19)
	Phang Nga	Phang Nga	Khao Chong	Khao Chong	Sakaerat	Sakaerat	Sakaerat	Sakaerat	Chiang Mai	Tanintharyi
	Thailand	Thailand	Thailand	Thailand	Thailand	Thailand	Thailand	Thailand	Thailand	Myanmar
	non-type	non-type	non-type	non-type	non-type	non-type	non-type	non-type	non-type	non-type
sex	m	f	f	f	m	m	m	m	m	f
supralabials (SU)	10	9	9	10	10	9	10	10	10	10
infralabials (IL)	11	11	11	10	12	11	11	11	11	11
supra-auricular lobe	small ridge	small ridge	small ridge	small ridge	small ridge	small ridge	small ridge	small ridge	small ridge	small ridge
midbody transverse dorsals (MB)	85	80	82	89	89	95	94	95	90	87
midbody transverse ventral scales (VS)	30	32	30	31	32	35	32	37	35	30
enlarged pore-bearing precloacal scales in males (PP)	21	/	/	/	20	20	20	24	21	/
enlarged precloacal scales (PS)	23	20	18	20	22	20	22	24	21	21
enlarged post-precloacal scale rows (PPS)	5	4	5	6	6	5	5	5	6	6
transversely expanded 4th toe lamellae (TL4)	16	16	13	14	15	14	14	14	16	13
scales across widest portion of caudal flap (CF)	/	/	/	28	/	/	30	33	/	/
edges of caudal flap smooth or crenulated	/	/	/	/	/	/	/	/	/	/
thick postorbital marking	no	no	no	no	no	yes	no	no	no	yes
irregularly shaped, white vertebral markings	no	no	no	no	no	no	no	no	no	no
SVL	78.4	87.1	76.8	78.5	72.4	73.6	87.2	81.1	80.2	92.0
TL	78.0r	71.5r	20.7b	75.0	66.7r	45.8	82.0	75.7	73.5r	52.0r
TW	7.0	7.5	6.2	6.9	6.1	7.4	7.1	7.4	7.1	7.7
HL	22.0	23.5	20.2	21.7	21.7	20.3	24.8	22.2	22.5	25.9
HW	19.4	18.4	15.2	15.9	15.4	15.7	17.4	16.4	16.2	17.8
HD	8.8	10.8	8.0	8.7	8.1	8.4	10.0	10.0	10.1	11.0
SNL	10.3	10.9	8.7	8.7	9.7	10.2	10.8	10.0	10.2	11.5
ED	5.1	5.5	4.8	9.6	4.9	/	5.1	4.6	5.4	5.7
TD	2.3	1.8	2.2	1.91	1.5	2.0	2.2	2.6	2.2	2.2
IN	4.3	3.3	3.1	1.7	2.6	3.2	2.8	3.5	3.0	/
IO	8.3	8.4	7.7	7.8	7.7	8.5	9.1	8.7	8.6	8.5
AXG	38.1	46.4	32.8	36.0	32.9	34.4	42.1	38.8	33.0	44.0
FL	8.9	10.2	8.0	9.9	9.2	9.3	11.1	8.1	9.14	11.0
TBL	12.7	13.7	11.9	12.3	11.0	11.9	14.1	13.4	13.3	15.3

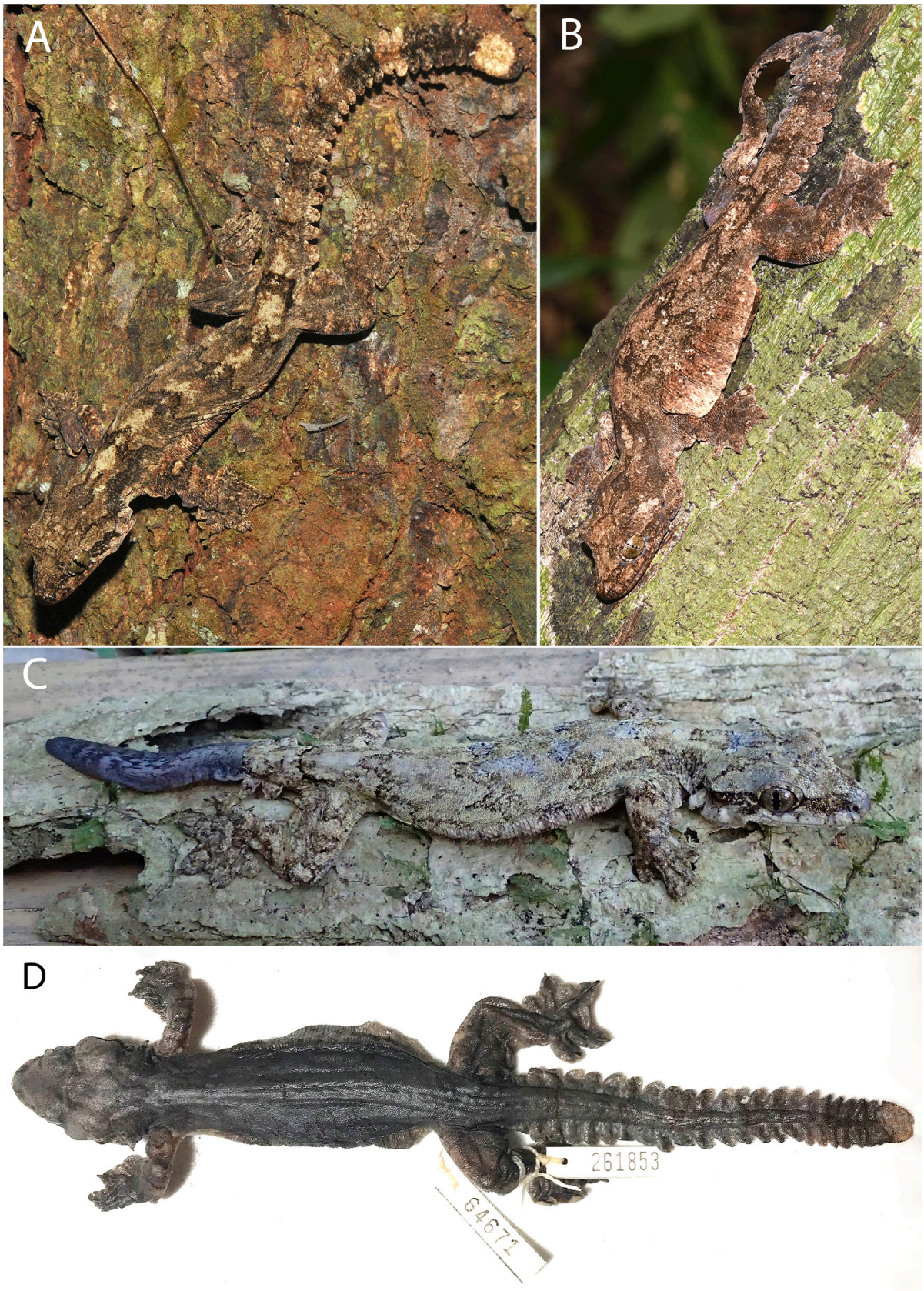

FIGURE 12. *Ptychozoon tokehos* **sp. nov.** A. CBC 1217 from Phnom Samkos, Pursat Province, Cambodia. Photograph by Neang Thy. B. Paratype CBC 03162 from Bokor National Park, Teuk Chou District, Kampot Province, Cambodia. Photograph by Neang Thy. C. USNM 587523 from Lenya National Park, Tanintharyi Region, Myanmar. Photograph by D. Mulcahy. D. Holotype FMNH 261853 from Kirirom National Park, Phnom Sruoch District, Kampong Speu Province, Cambodia. Photograph by L. L. Grismer.

FIGURE 13. Forest habitat of *Ptychozoon tokehos* **sp. nov.** A. Phnom Samkos, Pursat Province, Cambodia. B. Bokor National Park, Teuk Chou District, Kampot Province, Cambodia. Photographs by L. L. Grismer.

Tail original, flattened, shorter than SVL (TL/SVL 0.88); two median rows of transversely widened, smooth subcaudals anteriorly becoming less regular and broken up posteriorly; postcloacal scales large, flat, imbricate; dorsal caudals flat, juxtaposed, larger than dorsal body scales, bearing whorls of larger scales; tail width and caudal lobes decrease posteriorly; 22 caudal lobes on each side slightly angled posteriorly; and tail terminates in a short, narrow flap (10.0 mm) bearing smooth edges.

Dark phase coloration in life (Fig. 12). Dorsal ground color of head, body, and tail brown; top of head darkly speckled; darker, inverted Y-shaped marking overlying nape and occiput; labial scales lighter than body, delimited by thin, dark lines at their junctures; infra-auricular flap same color as labials; irregularly shaped, white, vertebral markings between and just posterior to the forelimb insertions and in the sacral region; four faint, thin, deeply sinuous dorsal bands between limb insertion transitioning into approximately five wide, faint, caudal bands; terminal caudal band on caudal flap dull-white; subcaudal region mottled, weakly banded; iris bronze; gular region, throat, ventral surfaces of limbs, pectoral region, and belly dull-white with stippled scales. In preservation, the coloration is uniformly dull-grey on all dorsal surfaces with only faint patterning visible.

Variation (Fig. 12). Variation in coloration and pattern is highly variable due to this species' having dark and light color phases and its ability to substrate match. Color pattern variation in the paratypes described here is based on preserved and living material. The paratypes closely approximate the holotype in all aspects coloration and pattern. Caudal banding is present in all specimens in varying degrees of distinctness. FMNH 261852–53 have a series of large, irregularly shaped, white, vertebral markings extending from the nape to the postsacral region whereas no other specimens (N=17) have these markings. FMNH 261852 and 261854 have partially regenerated tails bearing a single flap with no lobes. FMNH 177359, 181844, and 261851 are males bearing 23, 22, and 21 pore-bearing precloacal scales. Variation in meristic characters is presented in Table 8.

Comparisons (Tables 4, 5; Figs. 3, 5, 6). Differences between *Ptychozoon tokehos* **sp. nov.**, *P. kabkaebin* **sp. nov.**, and *P. cicakterbang* **sp. nov.** are listed above in the comparisons sections of those species. *Ptychozoon tokehos* **sp. nov.** differs from *P. intermedium, P. kuhli,* and *P. trinotaterra* in lacking, as opposed to having, caudal tubercles. From *P. intermedium, P. nicobarense, P. rhacophorus, P. trinotaterra,* and *P. kaengkrachanense* it differs in having four body bands as opposed to 0–3. *Ptychozoon tokehos* **sp. nov.** differs from *P. bannaense, P. horsfieldii, P. intermedium, P. kuhli, P. nicobarense, P. rhacophorus, P. trinotaterra,* and *P. kaengkrachanense* in having an emargination between the pre-antebrachial flap and digit I as opposed to no emargination. From *P. popaense* it differs by having a maximum SVL of 97.5 mm versus 86.2 mm. *Ptychozoon tokehos* **sp. nov.** is well-separated from *P. cicakterbang* **sp. nov.** and *P. lionotum* in the PCA and from all species in the DAPC where their 95% confidence ellipses do not overlap. *Ptychozoon tokehos* **sp. nov.** occupies a significantly different position along PC1 from that of *P. cicakterbang* **sp. nov.** and along PC2, it occupies a significantly different positon from those of *P. kabkaebin* **sp. nov.** and *P. lionotum.* From all other species of the *P. lionotum* group it is further separated by an uncorrected pairwise sequence divergence of 4.1–15.5%. Combinations of other characters differentiating *P. kabkaebin* **sp. nov.** from other more distantly related species are presented in Table 5.

Distribution (Fig. 1). *Ptychozoon tokehos* **sp. nov.** has a circum-Gulf of Thailand distribution extending from Cat Tien, Dong Nai Province and Phu Quoc Island, Kien Giang Province in southern Vietnam (Nguyen *et al.* 2009), across the mountainous Cardamom region of southern Cambodia and eastern Thailand, around the Chao Phraya Basin and southward down the Thai-Malay Peninsula of Thailand and Myanmar to at least Hat Yai, Songkla Province, Thailand. Nguyen *et al.* (2009) report *P. tokehos* **sp. nov.** from Trang Bom, Dong Nai Province, in southern Vietnam based on an illustration in Bourret (2009; Fig. 39.) The specimen illustrated however, has three body bands instead of four indicating it may be *P. trinotaterra.* We have examined photographs of specimens from southern Thailand near the Thai-Malay border from Hat Yai, Songkla (LUSDPC 10946) and Muang Trat, Trat (LSUDPC 10947) that we consider *P. tokehos* **sp. nov.** and not *P. cicakterbang* **sp. nov.** as they have a weak supra-auricular ridge as opposed to a prominent supra-auricular lobe. Confirmation awaits the examination of these specimens (Grismer *et al.* in prep).

Etymology. The specific epithet *tokehos* is the Khmer (Cambodian) word used for *Ptychozoon.*

Natural history. *Ptychozoon tokehos* **sp. nov.** is a forest-dwelling species found in hilly areas from sea level to at least 700 m in elevation. This species does quite well in disturbed forests and is commonly found on man-made structures. The holotype and paratypes from Kirirom National Park (FMNH 261851–54) were all found during the day (1400–1630 h) on or near the exterior walls of a building on a grassy plateau within open pine forest. FMNH 261851 was found on the branch of a large tree abutting an exterior wall, FMNH 261852 was found beneath a layer

of paint peeling off the exterior wall of the building approximately 2.5 m above the ground, and FMNH 261853–54 were found on the exterior walls. Pauwells *et al.* (2000) noted that MNHN 1998.590 and 1999.7661 from Phang-Nga were collected from walls inside a forestry department office building where other juveniles and adults were seen. They also observed other specimens inside houses and on the outside of cages in a zoo. MNHN 1999.7661 was carrying two eggs. Additionally they found a pair of the eggs 1.6 m above the ground glued to a tree in evergreen forest of which one contained a fully formed embryo. These observations indicate that the reproductive season of *P. tokehos* **sp. nov.** in southern Thailand occurs during mid-February. All paratypes from Bokor National Park (CBC 03162, NCSM 98986–87; Fig. 13) were found at night approximately 1.3 m above the ground on the trunks of trees along a trail in disturbed evergreen forest between 315 m and 328 m in elevation. The paratype FMNH 18144 and additional specimens from Sakaerat (FMNH 181823–24, 181828–29) were collected from an undisturbed lowland forest at approximately 16 m in elevation. The Tanintharyi specimen (USNM 587523) was collected from the trunk of a tree along a logging road in secondary forest at 58 m in elevation. The paratype and additional specimens (FMNH 177358–59, 177550) from Khao Chong, Thailand were all collected from primary forest at approximately 130 m in elevation. A hatchling (FMNH 177360) from Khao Chong was collected during June.

Ptychozoon lionotum Annandale, 1905
Burmese Parachute Gecko
Fig. 14

Ptychozoon homalocephalum var. *lionotum* Annandale, 1905:31
Ptychozoon homalocephalum Var. *lionatum* (sic.) Das, Dattagupta, & Gayen 1998:133

Syntypes. ZSI 2601–02. The type locality for *Ptychozoon lionotum* is commonly listed as "Pegu" (Annandale 1905; Smith 1935; Uetz *et al.* 2019). At the time of its description, Pegu was the name of the administrative district that covered a broad area of the southern one-third of the Ayeyarwady Basin, Myanmar where the collector, Signor L. Fea (Fea 1897), obtained a single male specimen (one of the syntypes). Earlier, however, Boulenger (1893:316) noted that Fea's specimen came from "Palon" which according to Grismer *et al.* (2018b), is the town of Hpa Lon, Yangon Region. Hpa Lon was also noted as the type locality for *Cyrtodactylus peguensis* Boulenger, 1893 which was restricted to the "Myin Mo Swhe Taung Pagoda, Yangon Division, Taikkyi Township, Yangon (north) District, Myanmar", 9.5 km to the east as this was the closest suitable hilly habitat for *C. peguensis*. However, being that *Ptychozoon* are commonly found on walls and other surfaces on man-made structures, especially in rural areas, it is conceivable that the specimen was collected in the village of Hpa Lon and thus, we restrict the type locality to Hpa Lon, Taikkyi Township, Yangon (north) District, Yangon Division, Myanmar (17.44552°N 95.91485°E, 20 m in elevation; Fig. 1). Annandale (1905) reported on three specimens from "Pegu" that he considered conspecific and apparently allocated two of them as syntypes. We presume one of those was the specimen collected by Signor L. Fea and reported on by Boulenger (1893). We do not know which of the other specimens is the second syntype.

Diagnosis. *Ptychozoon lionotum* differs from all other species of *Ptychozoon* by having the following unique combination of characters: a maximum SVL of 95.9 mm; supranasals not in contact; 7–9 supralabials; 9–11 infralabials; infra-auricular cutaneous flap present; absent to weak supra-auricular ridge; no dorsal or caudal tubercles; imbricate parachute support scales on dorsal surface of patagia; no prominently raised ridges on ventral surface of patagia; 73–81 midbody dorsal scales; 35–38 ventral scales; an emargination between the pre-antebrachial flap and digit I; no enlarged femoral scales; 20–22 pore-bearing precloacal scales in males; 23 or 24 enlarged precloacal scales; five rows of enlarged post-precloacal scales; 16 or 17 transverse subdigital lamellae on the fourth toe; slightly enlarged dorsal caudal scales forming intermittent whorls weak to absent; approximately 29–34 scales across the widest portion of the caudal flap; distal lobes fusing to form a short, narrow, caudal flap; edges of caudal flap smooth; caudal lobes angled posteriorly; caudal lobes showing minimal posterior reduction in size; postorbital striping variable; four dark body bands between limb insertions; and irregularly shaped, white, vertebral markings (Tables 4, 5, 9).

Distribution (Fig. 1). *Ptychozoon lionotum* ranges from Tad Kuang Si, Luang Phabang Province in northeastern Laos, west to Chin Minbyin Village, on Ramree Island, Rakhine State, in southwestern Myanmar and northward to south Mizoram in eastern India (Pawar & Biswas 2001).

TABLE 9. Character state matrix for *Ptychozoon lionotum* and *P. trinotaterra* for the newly discovered localities.

	NCSM 79474 (36) *lionotum* Tad Kuang Si Laos	NCSM 79473 (36) *lionotum* Tad Kuang Si Laos	CAS 238865 (39) *lionotum* Rakkine Myanmar	CAS 221168 (37) *lionotum* Bago Divisiom Myanmar	NCSM 77915 *trinotaterra* Nakai Nam Theun Laos	FMNH 177549 *kaengkrachanense* Chiang Mai Thailand
sex	m	f	m		m	m
supranasals in contact	no	no	no	no	yes	no
supralabials to middle of eyeball (SU)	9	9	7	9	7	9
infralabials (IL)	10	11	9	11	8	10
infra-auricular cutaneous flap present	yes	yes	yes	yes	yes	yes
supra-auricular lobe	absent	weak ridge	weak ridge	weak ridge	absent	weak ridge
dorsal and caudal tubercles	absent	absent	absent	absent	present	absent
imbricate parachute support scales	present	present	present	present	present	present
midbody transverse dorsal scales (MB)	76	81	73	73	81	79
midbody transverse ventral scales (VS)	38	35	35	35	28	30
space between pre-antebrachial flap and digit I	yes	yes	yes	yes	no	no
enlarged femoral scales	absent	absent	absent	absent	absent	absent
enlarged pore-bearing precloacals in males (PP)	22	/	20	/	17	15
enlarged precloacal scales (PS)	24	24	23	23	17	17
enlarged post-precloacal scale rows PPS)	5	5	5	5	5	7
transversely expanded 4th toe lamellae (TL4)	16	17	16	17	13	12
scales across widest portion of caudal flap (CF)	/	34	29	/	/	/
distal caudal lobes fused into short caudal flap	/	yes	yes	/	/	/
edges of caudal flap smooth or crenulated	/	smooth	smooth	/	/	/
caudal lobe angling	/	slightly	slightly	/	/	/
tail and caudal lobes with distal reduction	/	no	no	/	/	/
thick postorbital stripe	/	yes	no	no	yes	yes
bands between limb insertions	/	4	4	4	3	3
irregularly shaped, white vertebral markings	yes	yes	yes	yes	yes	no

.....continued on the next page

TABLE 9. (Continued)

	NCSM 79474 (36) *lionotum* Tad Kuang Si Laos	NCSM 79473 (36) *lionotum* Tad Kuang Si Laos	CAS 238865 (39) *lionotum* Rakkine Myanmar	CAS 221168 (37) *lionotum* Bago Division Myanmar	NCSM 77915 *trinotaterra* Nakai Nam Theun Laos	FMNH 177549 *kaengkrachanense* Chiang Mai Thailand
SVL	89.2	95.9	79.1	81.5	71.1	78.7
TL	71.4	106.5	85.7	/	52.6r	/
TW	8.01	9.60	7.3	/	8.6	8.8
HL	86.0	27.2	20.3	22.5	19.2	21.6
HW	75.4	20.8	16.3	18.5	14.5	17.5
HD	24.6	10.5	8.6	9.5	8.3	10.4
SNL	18.4	13.1	8.7	9.6	7.5	9.5
ED	9.2	4.9	4.6	4.7	4.4	5.1
TympD	11.6	1.6	2.0	1.3	2.3	2.3
IN internarial	5.0	3.3	3.0	2.9	2.6	3.2
IO interorbital	2.1	2.6	8.2	8.5	1.6	8.0
AGD	3.1	48.9	35.5	35.9	34.4	39.2
FL	22.0	22.6	9.4	16.7	10.10	9.5
TBL	16.7	16.3	13.2	13.7	12.0	13.5

Natural history. The specimens collected from the Tad Kuang Si Provincial Protected Area, Laos (NSCM 79473–74; Fig. 15) were caught at night in semi-evergreen forest 1.5–2 m above the ground on the trunks of large trees. CAS 238865 from Chin Minbyin Village in Myanmar was collected at 1100 hrs approximately 2 m above the ground on a tree. CUMZ.2005.07.30.40 from Khao Luang, Surat Thani Province, Thailand was found on the trunk of a tree at night facing head down approximately 30 cm above the ground.

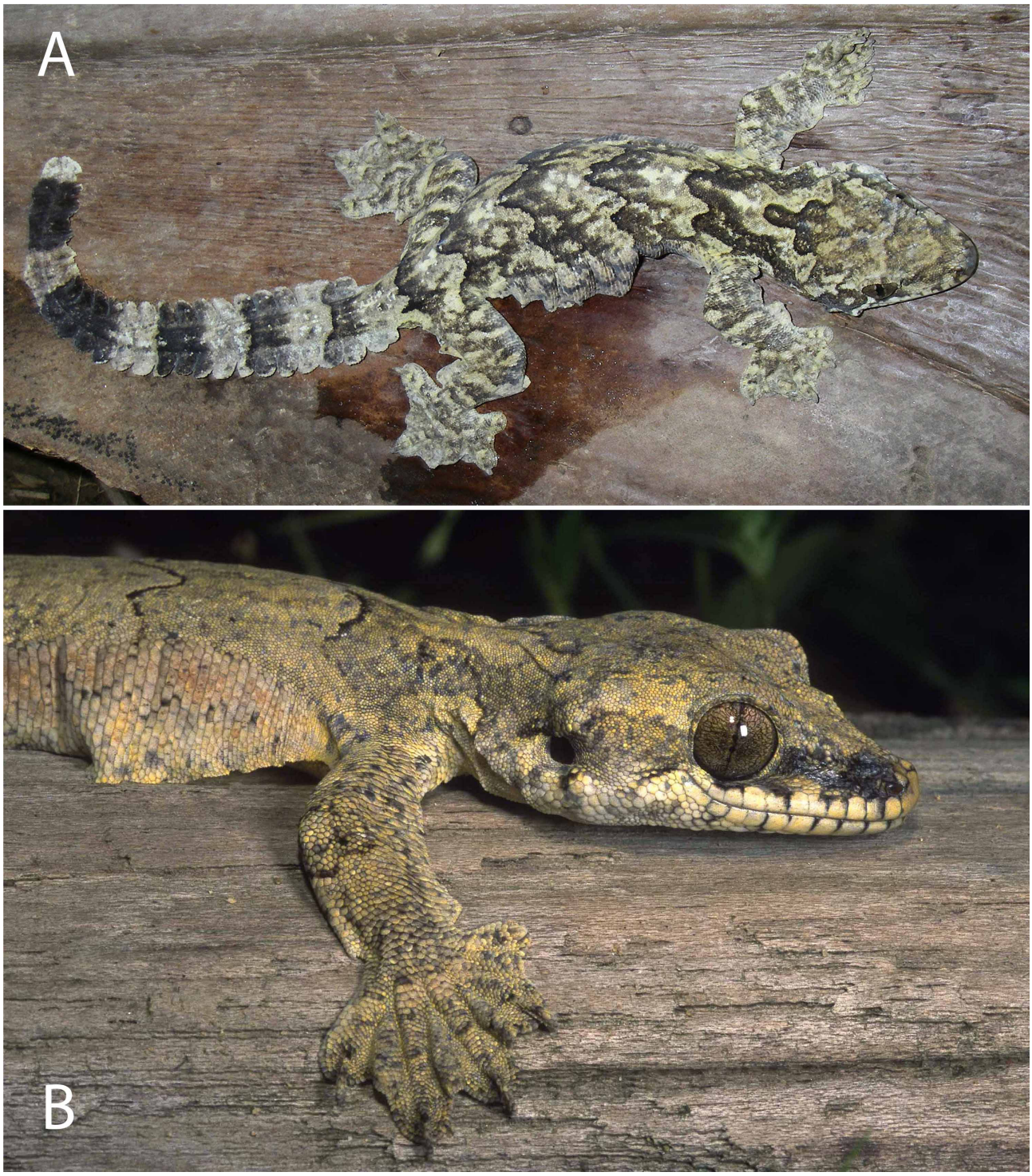

FIGURE 14. *Ptychozoon lionotum*. A. NCSM 79473 from Tad Kuang Si, Luang Prabang Province, Laos. Photograph by B. L. Stuart. B. CAS 238865 Rakhine State, Myanmar. Photograph by Myanmar Herpetological Survey.

FIGURE 15. Forest habitat of *Ptychozoon lionotum* at Tad Kuang Si, Luang Prabang Province, Laos. Photograph by B. L. Stuart.

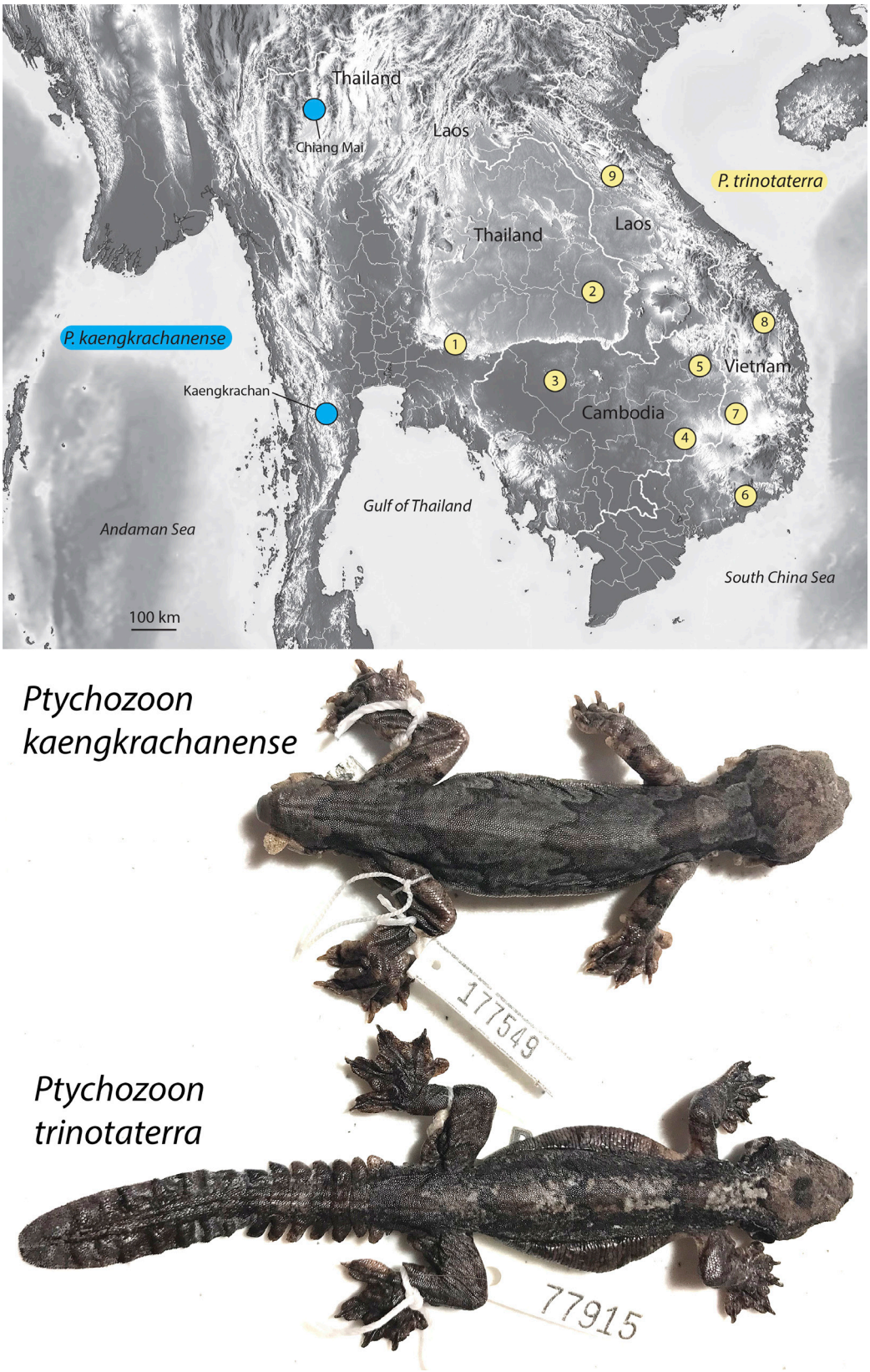

FIGURE 16. Locality data (map) and new distributional records for *Ptychozoon kaengkrachaense* (Sumontha *et al*. 2012) and *P. trionotaterra*. Thailand: 1. Type locality in Nakhon Ratchasima Province (Brown 1999); 2. Ubon Ratchathani Province (Kunya *et al*. 2011). Cambodia: 3. Siem Reap Province (Hartmann *et al*. 2014); 4. Keo Seima, Mondulkiri Province (LSUDPC 10961) newly reported here. 5. Ratanakiri Province (LSUDPC 10962) newly reported here. Vietnam: 6. Dong Nai province (Nguyen *et al*. 2009); 7. Dak Lak Province (Brown 1999); 8. Gia Lai Province (Brown 1999). Laos: 9. Nakai-Nam Theun, Khammouan Province (NCSM 77915) newly reported here.

Notes on the distribution of *Ptychozoon kaengkrachanense* and *P. trinotaterra*

Brown *et al.* (2012) recovered *Ptychozoon trinotaterra* as the sister species of *P. kuhli* in their phylogenetic analysis which is confirmed here with an additional specimen NCSM 77915 (Figs. 2, 16) from a new locality in Laos. NCSM 77915 was collected in Nakai-Nam Theun National Protected Area, WMPA headquarters, Nakai District, Khammouan Province, Laos (17.50500°N 105.14639°E) on 10 November 2007 by William G. Robichaud and represents a range extension of 245 km to the north from Ubon Ratchathani Province, Thailand (Kunya *et al.* 2012; Fig. 16) and the first confirmed account of this species for Laos. NCSM 77915 bears the combination of diagnostic characters that separate it from *P. lionotum* (see Brown 1999) by having three versus four dark-colored dorsal body bands, 28 versus 35–38 ventral scales, 17 versus 20–22 pore-bearing precloacal scales in males, 17 versus 23 or 24 enlarged precloacal scales, 13 versus 16 or 17 subdigital lamellae on the fourth toe, paired middorsal caudal tubercles versus no caudal tubercles, no emargination between the pre-antebrachial flap and digit I versus having an emargination, and a 71.1 mm maximum SVL versus a 95.9 maximum SVL (Table 9). We examined photographs of two additional specimens, LSUDPC 10961 from Keo Seima, Mondulkiri and LSUDPC 10962 from Ratanakiri (exact locality not provided), that had three bands between the limb insertions that we consider to represent new localities for *P. trinotaterra* in Cambodia (Fig. 16).

A second specimen (FMNH 177549; Fig. 16) from Chiang Mai, Chiang Mai Province, Thailand (18.70585°N 98.98350°E, 299 m in elevation) was cataloged as *P. lionotum*. FMNH 177549 bears the combination of diagnostic characters that separate it from *P. lionotum* (Brown 1999) in having three versus four dorsal body bands, 30 versus 35–38 ventral scales, 15 versus 20–22 pore-bearing precloacal scales in males, 17 versus 23 or 24 enlarged precloacal scales, 12 versus 16 or 17 subdigital lamellae on the fourth toe, no emargination between the pre-antebrachial flap and digit I versus an emargination being present, and a 78.7 mm maximum SVL versus a 95.9 maximum SVL (Table 9). Although these characters align this specimen with *P. kaengkrachanense* (Sumontha *et al.* 2012) we consider this identification tentative. The tail is missing so caudal tuberculation could not be evaluated. FMNH 177549 may represent a considerable range extension of 629 km to the north from the type locality of Kaeng Krachan National Park, Phetchaburi Province, Thailand (Fig. 16). At this point we consider this specimen less likely to belong to *P. bannaense* from Yunnan Province, China approximately 390 km to the northwest in that it has 15 vs 17 (n=1) pore-bearing precloacal scales and a SVL of 71.1. mm versus 83.2–87.2 (n=2). Its specific confirmation must await additional specimens and a molecular analysis.

Discussion

Ptychozoon lionotum s.l. is demonstrated here to be a paraphyletic species complex composed of four deeply divergent, diagnosable, allopatric lineages and like so many "species" that were originally purported to range throughout large areas of Indochina (*e.g.* Stuart *et al.* 2006; Malhotra *et al.* 2011; Sheridan & Stuart 2018; Murdoch *et al.* 2019), this was more of an expectation than a surprise. Unlike other Indochinese gekkonid lineages that manifest cladogenic turnover across well-known biogeographic barriers (*e.g.* Agarwal *et al.* 2014; Grismer *et al.* 2017, 2018a,b; Grismer & Davis 2018), this is not always the case in the *P. lionotum* group. As noted above, *P. lionotum* extends approximately 1100 km from western Laos to Ramree Island in southwestern Myanmar and in so doing, crosses the Tenasserim Mountains that separate Thailand and Myanmar, the Sagaing Fault between the Eastern Yoma Mountains and Ayeyarwady Basin, and the entire southern section of the Ayeyarwady Basin (Fig. 1). These are known regions of cladogenic turnover in a number of other gekkonid lineages, namely *Cyrtodactylus* (Agarwal *et al.* 2014; Grismer *et al.* 2018a,b) and *Hemiphyllodactylus* (Grismer *et al.* 2017; Grismer & Davis 2018). Yet the uncorrected pairwise sequence divergence among individuals (n=4) of *P. lionotum* is 0.00% (Fig. 3). At this juncture, we have no logical hypothesis to explain this unexpected phylogeographic pattern. Conversely, modest phylogeographic structure occurs within *P. tokehos* **sp. nov.** USNM 587523 from Tanintharyi, Myanmar north of the Isthmus of Kra in southern Thailand and CUMZ.2005.07.30.40 from Khao Luang immediately south of the Isthmus of Kra (Fig. 1) are separated by approximately 250 km and a sequence divergence of 5.2%. Sequence divergence between USNM 587523 and CUMZ.2005.07.30.40 and the Cardamom Mountain specimens in Cambodia (FMNH 261852, CBC 0316, NCSM 98986–87) across the Gulf of Thailand ranges from 4.1–6.2% (Fig. 3). The upper and lower ranges of divergence within *P. tokehos* **sp. nov.** will likely be extended with additional sampling from the intervening areas

as well as Chiang Mai, Thailand and the Pattani region between Khao Luang and the Thai-Malay border (Fig. 1). This may require additional taxonomic changes (Grismer *et al.* in prep.). *Ptychozoon cicakterbang* **sp. nov.** shows significant genetic divergence amongst some of its populations that does not correspond to geography. For example, LSUHC 5539, 5597, and 11894 collected within 100 m of one another along the same trail on the small Island of Sibu off the southeast coast of Peninsular Malaysia share a sequence divergence among them of 7.2–8.2%. Whereas LSUHC 11418, 11419, and 11439 from the small island of Bidong off the northwest coast are genetically identical. It may be that Sanger sequencing has reached its descriptive limits within *P. cicakterbang* **sp. nov.** and that a phylogenomic data set will be needed to resolve these apparent inconsistencies. The phylogeographic break between *P. cicakterbang* **sp. nov.** and (*P. popaense,* (*P. tokehos* **sp. nov.** ((*P. lionotum* + *P. kabkaebin* **sp. nov.**))) occurs across the Kangar-Pattani Line on the Thai-Malay border region which is an established biogeographic region of lineage turnover for many other species (see Grismer 2011a; Grismer *et al.* 2014; Grismer *et al.* 2019; Quah & Anuar 2018 and references therein).

Given that new species of *Ptychozoon* are being discovered as a result of field work in remote areas (Sumontha *et al.* 2012; Wang *et al.* 2016; Grismer *et al.* 2018a) and their phylogeny is composed of diagnosable species separated by long branches with divergences of 4.1–15.5% within the *lionotum* group and up to 17.5% among all *Ptychozoon*, suggests that it is very likely that more species have yet to be discovered. Given their ability to substrate match, it is not surprising that many populations are known from only a few specimens and many of these were seen only because they were low on the trunks of trees in cleared, open areas or on man-made structures (Brown *et al.* 1997; Brown 1999; Das & Vijayakumar 2009; Grismer 2011a; Kunya *et al.* 2011; Sumontha *et al.* 2012; Herr & Lee 2016; Wang *et al.* 2016; Fitzsimons 2017; Grismer *et al.* 2018a). Continued field work and tissue sampling throughout Indochina should recover additional species and fill in distribution gaps within known species and illuminate clearer biogeographic patterns.

Acknowledgments

We are grateful to the following museum curators for the loan of specimens: Alan Resetar (FMNH), Annmarie Ohler and Patrick David (MNHN), Kevin deQueiroz (USNM), and Lauren Schienberg (CAS). We wish to thank Anchelee AowPhol, Alexandre Teynie, and Ulrich Manthey for photographs of specimens they encountered in the field. ESHQ would like to thank the Department of Wildlife and National Parks, Peninsular Malaysia for issuing us a research permit (P-00074-15-18) to conduct research in Malaysia and his research is partially supported by the USM postdoctoral scheme. RMB's work was supported by NSF DEB 0743491, 1654388, and 1418895. Dara An, Joe Walston, William G. Robichaud, and Jennifer A. Sheridan assisted BLS with fieldwork in Cambodia and Laos. Fieldwork in Laos by BLS, SP, NS and SS was supported by grants from the John D. and Catherine T. MacArthur Foundation (grants 03-75621 and 92482-0), and the U.S. National Science Foundation (grant DEB-1145922), with logistical support provided by the Wildlife Conservation Society Laos Program, and specimen export permits provided by the Ministry of Agriculture and Forestry, Vientiane. Fieldwork by BLS and NT in Cambodia was supported by grants from the National Geographic Society (grants 6247-98 and WW-R016-17) with logistical support provided by the Wildlife Conservation Society Cambodia Program and Wild Earth Allies Cambodia Program, and specimen export permits provided by the Ministry of Environment, Phnom Penh. We thank He Say Samal, Minister of Environment of Cambodia for fieldwork and export permits. DGM's Tanintharyi, Myanmar field work was made possible with the help of Frank Momberg and Mark Grindley (Fauna & Flora International), Melissa Songer (Smithsonian Conservation Biology Institute), and support of the Myanmar Forest Department of the Ministry of Natural Resources and Environmental Conservation. Portions of lab and computer work were conducted with the support of the Laboratories of Analytical Biology facilities of the NMNH and was partially funded by the Global Genome Initiative (NMNH) grant GGI-Peer-2015 (028).

References

Acinas, S.G., Klepac-Ceraj, V., Hunt, D.E., Pharino, C., Ceraj, I., Distel, D.L. & Polz, M.F. (2004) Fine-scale phylogenetic architecture of a complex bacterial community. *Nature*, 430, 551–554. https://doi.org/10.1038/nature02649

Agarwal, I., Bauer, A.M., Jackman, T.R. & Karanth, K.P. (2014) Insights into Himalayan biogeography from geckos: a molecular phylogeny of *Cyrtodactylus* (Squamata: Gekkonidae). *Molecular Phylogenetics and Evolution*, 80, 145–155. https://doi.org/10.1016/j.ympev.2014.07.018

Annandale, N. (1905) Notes on some Oriental geckos in the Indian Museum, Calcutta, with descriptions of new forms. *Annals & Magazine of Natural History*, Series 7, 15, 26–32. https://doi.org/10.1080/03745480509443635

Barraclough, T.G., Birky, C.W. Jr. & Burt, A. (2003) Diversification in sexual and asexual organisms. *Evolution*, 57, 2166–2172. https://doi.org/10.1554/02-339

Boulenger G.A. (1893) Concluding report on the reptiles and batrachians obtained in Burma by Signor L. Fea, dealing with the collection made in Pegu and the Karin Hills in 1887–88. *Annali del Museo civico di storia naturale di Genova*, 2, 304–345.

Boulenger, G.A. (1899) Description of three new reptiles and a new batrachian from Mt. Kina Balu, North Borneo. *Annals and Magazine of Natural History*, 4, 451–453. https://doi.org/10.1080/00222939908678228

Boulenger, G.A. (1912) *A vertebrate fauna of the Malay Peninsula from the Isthmus of Kra to Singapore including the adjacent islands*. Reptilia and Batrachia. Taylor & Francis, London, 294 pp. https://doi.org/10.5962/bhl.title.10813

Bourret, R. (2009) *Les Lézards de L'Indochine*. Edition Chimaira, Frankfurt am Main, 624 pp. [2009 reprinting]

Brown, R.M. (1999) New species of parachute gecko (Squamata: Gekkonidae: genus *Ptychozoon*) from northeastern Thailand and central Vietnam. *Copeia*, 1999, 990–1001. https://doi.org/10.2307/1447974

Brown, R.M., Diesmos, A.C. & Oliveros, C.H. (2011) New flap-legged forest gecko (Genus *Luperosaurus*) from the Northern Philippines. *Journal of Herpetology*, 45 (2), 202–210. https://doi.org/10.1670/10-123.1

Brown, R.M, Ferner, J.W. & Diesmos, A.C. (1997) Definition of the Philippine parachute gecko, *Ptychozoon intermedium* Taylor 1915 (Reptilia: Squamata: Gekkonidae): redescription, designation of a neotype, and comparisons with related species. *Herpetologica*, 53, 357–373.

Brown, R.M., Siler, C.D., Grismer, L.L., Das, I. & McGuire, J.A. (2012) Phylogeny and cryptic diversification in Southeast Asian flying geckos. *Molecular Phylogenetics and Evolution*, 65, 351–361. https://doi.org/10.1016/j.ympev.2012.06.009

Brown, R.M., Supriatna, J. & Ota, H. (2000) Discovery of a new species of *Luperosaurus* (Squamata: Gekkonidae) from Sulawesi, with a phylogenetic analysis of the genus, and comments on the status of *Luperosaurus serraticaudus. Copeia*, 2000, 191–209. https://doi.org/10.1643/0045-8511(2000)2000[0191:doanso]2.0.co;2

Cangelosi, R. & Goriely, A. (2007) Component retention in principal component analysis with application of cDNA microarray data. *Biology Direct*, 2, 2. https://doi.org/10.1186/1745-6150-2-2

Cantor, T.E. (1847) Catalogue of reptiles inhabiting the Malayan Peninsula and islands, collected or observed by Theodore Cantor, Esq., M.D. Bengal Medical Services. *Journal of the Asiatic Society of Bengal*, 16, 607–656 + 897–952 + 1026–1078. https://doi.org/10.5962/bhl.title.5057

Chan-ard, T., Grossmann, W., Gumprecht, A. & Schultz, K.-D. (1999) *Amphibians and Reptiles of Peninsular Malaysia and Thailand.* Bushmaster Publications, Wuerselen, 240 pp. https://doi.org/10.15560/10.2.335

Chiari, Y. & Claude, J. (2012) Morphometric identification of individuals when there are more shape variables than reference specimens: A case study in Galápagos tortoises. *Comptes Rendus Biologies*, 355, 62–68. https://doi.org/10.1016/j.crvi.2011.10.007

Cox, M.J., van Dijk, P.P., Nabhitabhata, J. & Thirakhupt, K. (1998) *A Photographic Guide to Snakes and Other Reptiles of Peninsular Malaysia, Singapore and Thailand*. New Holland Publishers (UK) Ltd., London, 144 pp. https://doi.org/10.2307/1447416

Coyne, J.A. & Orr, H.A. (1998) The evolutionary genetics of speciation. *Philosophical Transactions of the Royal Society of London B*, 353, 287–305. https://doi.org/0.1098/rstb.1998.0210

Das, I., Dattagupta, B. & Gayen, N.C. (1998) History and catalogue of reptile types in the collection of the Zoological Survey of India. *Journal of South Asian Natural History*, 3, 121–172.

Das, I. & Vijayakumar, S.P. (2009) New species of *Ptychozoon* (Sauria: Gekkonidae) from the Nicobar Archipelago, Indian Ocean. *Zootaxa*, 2095, 8–20.

de Queiroz, K. (2007) Species concepts and species delimitation. *Systematic Biology*, 56, 879–886. https://doi.org/10.1080/10635150701701083

Dring, J.C.M. (1979) Amphibians and reptiles from northern Trengganu, Malaysia, with descriptions of two new geckos: *Cnemaspis* and *Cyrtodactylus*. *Bulletin of the British Museum* (*Natural History*), 34, 181–241.

Drummond, A.J., Ashton, B., Buxton, S., Cheung, M., Cooper, A., Duran, C., Field, M., Heled, J., Kearse, M., Markowitz, S., Moir, R., Stones-Havas, S., Sturrock, S., Thierer, T. & Wilson, A. (2011) *Geneious. Version 5.6*. Available from: http://www.geneious.com/ (accessed 20 May 2019)

Drummond, A.J., Suchard, M.A., Xie, D. & Rambaut, A. (2012) Bayesian phylogenetics with BEAUti and BEAST 1.7. *Molecular Biology and Evolution*, 29, 1969–1973. https://doi.org/10.1093/molbev/mss075

Dudley, R., Byrnes, G., Yanoviak, S.P., Borrell, B., Brown, R.M. & McGuire, J.A. (2007) Gliding and the functional origins of flight: biomechanical novelty of necessity? *Annual Review of Ecology, Evolution, and Systematic*s, 38, 179–201. https://doi.org/10.1146/annurev.ecolsys.37.091305.110014

Fea, L. (1897) Viaggio di Leonardo Fea in Birmania e regioni vicine. LXXVI. Riassunto generale dei risultati zoologici. *Annali del Museo Civico di Storia Naturale di Genova*, Series 2, 42, 383–660. https://doi.org/10.5962/bhl.part.16764

Fisher-Reid, M.C. & Wiens, J.J. (2011) What are the consequences of combining nuclear and mitochondrial data for phylogenetic analysis? Lessons from *Plethodon* salamanders and 13 other vertebrate clades. *BMC Evolutionary Biology*, 11, 1–20. https://doi.org/10.1186/1471-2148-11-300

Fitzsimons, J.A. (2017) Ecological notes on the three-banded parachute gecko *Ptychozoon trinotaterra* in southern Vietnam. *Russian Journal of Herpetology*, 24, 327–328. https://doi.org/10.1146/annurev.ecolsys.37.091305.110014

Fontaneto, D., Herniou, E.A., Boschetti, C., Caprioli, M., Melone, G., Ricci, C. & Barraclough, T.G. (2007) Independently evolving species in asexual bdelloid rotifers. *PLoS Biology*, 5, e87. https://doi.org/10.1371/journal.pbio.0050087

Fujisawa, T. & Barraclough, T.G. (2013) Delimiting species using single-locus data and the Generalized Mixed Yule Coalescent approach: a revised method and evaluation on simulated data sets. *Systematic Biology*, 62 707–724. https://doi.org/10.1093/sysbio/syt033

Gray, J.E. (1827) A synopsis of the genera of saurian reptiles in which some new genera are indicated, and the others reviewed by actual examination. *Philosophical Magazine, London*, 2, 54–58. https://doi.org/10.1080/14786442708675620

Gray, J.E. (1845) *Catalogue of the Specimens of Lizards in the Collection of the British Museum*. Trustees of die British Museum, London, xxvii + 289 pp. https://doi.org/10.5962/bhl.title.5499

Grismer, L.L. (2011a*) Lizards of Peninsular Malaysia, Singapore and their Adjacent Archipelagos*. Edition Chimaira, Frankfurt am Main, 728 pp.

Grismer, L.L. (2011b) *Amphibians and Reptiles of the Seribuat Archipelago*. Edition Chimaira, Frankfurt am Main, 129 pp.

Grismer, L.L., Chav, T., Neang, T., Wood Jr., P.L., Grismer, J.L., Youmans, T.M., Ponce, A., Daltry, J.C. & Kaiser, H. (2007) The herpetofauna of the Phnom Aural Wildlife Sanctuary and checklist of the herpetofauna of the Cardamom Mountains, Cambodia. *Hamadryad*, 31, 216–241.

Grismer, L.L. & Davis, H.R. (2018c) Phylogeny and biogeography of bent-toed geckos (*Cyrtodactylus* Gray) of the Sundaic swamp clade. *Zootaxa*, 4472 (2), 365–374. https://doi.org/10.11646/zootaxa.4472.2.9

Grismer, L.L., Grismer, J.L., Wood Jr., P.L., Ngo, V.T., Neang, T. & Chan, K.O. (2011) Herpetology on the fringes of the Sunda Shelf: a discussion of discovery, taxonomy, and biogeography. *In*: Schuchmann, K.-L. (Ed.), *Tropical Vertebrates in a Changing World*. Bonner Zoologische Monographien, Bonn, pp. 57–97.

Grismer, L.L., Neang, T., Chav, T. Wood Jr., P.L., Oaks, J.R., Holden, J., Grismer, J.L., Szutz, T.R. & Youmans, T.M. (2008) Additional amphibians and reptiles from the Phnom Samkos Wildlife Sanctuary in the northwestern Cardamom Mountains, Cambodia, with comments on their taxonomy and the discovery of three new species. *Raffles Bulletin of Zoology*, 56, 161–175.

Grismer, L.L. & Pan, K.A. (2008) Diversity, endemism, and conservation of the amphibians and reptiles of southern Peninsular Malaysia and its offshore islands. *Herpetological Review* 39, 270–281.

Grismer, L.L. & Quah, E.S.H. (2019) An updated and annotated checklist of the lizards of Peninsular Malaysia, Singapore, and their adjacent islands. *Zootaxa*, 4545 (2), 230–248. https://doi.org/10.11646/zootaxa.4545.2.4

Grismer, L.L., Wood, P.L. Jr., Myint, K.T., Grismer, M.S., Brown, R.M. & Stuart, B.L. (2018a) Geographically structured genetic variation in *Ptychozoon lionotum* (Squamata: Gekkonidae) and a new species from an isolated volcano in Myanmar. *Zootaxa*, 4514 (2), 202–214. https://doi.org/10.11646/zootaxa.4514.2.4

Grismer, L.L., Wood. Jr., P.L., Myint, K.T., Zin, T., Quah, E.S.H., Murdoch, M.L., Grismer, M.S., Lin, A., Kyaw, H. & Ngwe, L. (2017) Twelve new species of *Cyrtodactylus* Gray (Squamata: Gekkonidae) from isolated limestone habitats in east-central and southern Myanmar demonstrate high localized diversity and unprecedented microendemism. *Zoological Journal of the Linnean Society*, 182, 862–959. https://doi.org/10.1093/zoolinnean/zlx057

Grismer, L.L., Wood Jr., P.P., Quah, E.S.H., Murdoch, M.L., Grismer, M.S., Herr, M.W., Espinoza, R.E., Brown, R.M. & Lin, A.

(2018b) A phylogenetic taxonomy of the *Cyrtodactylus peguensis* group (Reptilia: Squamata: Gekkonidae) with descriptions of two new species from Myanmar. *PeerJ*, 6, e5575.
https://doi.org/10.7717/peerj.5575

Grismer L.L., Wood Jr., P.L., Shahrul, A., Awal, R., Norhayati, A., Muin, M., Sumontha, M.,

Grismer, J., Chan, K.O., Quah, E.S.H. & Pauwels, O.S.G. (2014) Systematics and natural history of Southeast Asian rock geckos (genus *Cnemaspis* Strauch, 1887) with descriptions of eight new species from Malaysia, Thailand, and Indonesia. *Zootaxa*, 3880 (1), 1–147.
https://doi.org/10.11646/zootaxa.3880.1.1

Grismer, L.L., Youmans, T.M., Wood Jr. P.L. & Grismer, J.L. (2006) Checklist of the herpetofauna of the Seribuat Archipelago, West Malaysia with comments on biogeography, natural history and adaptive types. *Raffles Bulletin of Zoology*, 54, 157–180.

Grismer, L.L., Zaharil, D., Muin, M.A., Quah, E.H., Karin, B.R., Anwar, S. & Freitas, E.S, (2019) A new skink of the genus *Subdoleseps* (Hardwicke & Gray, 1828) from Peninsular Malaysia. *Zootaxa*. [in press]

Hartmann, T., Betts, A.B., de Greef, S. & Ihlow, F. (2014) First record of the rare parachute gecko *Ptychozoon trinotaterra* Brown, 1999 from Cambodia. *Cambodia Journal of Natural History*, 1, 8–11.

Herr, M.W. & Lee, D.S. (2016) New provincial record and range extension of the parachute gecko *Ptychozoon lionotum* Annandale, 1905 in Cambodia, with notes on habitat use. *Cambodian Journal of Natural History*, 2, 111–113.

Heyer, W.R. & Pongsapipatana, S. (1970) Gliding speeds of *Ptychozoon lionatum* (Reptilia: Gekkonidae) and *Chrysopelea ornata* (Reptilia: Colubridae). *Herpetologica*, 26, 317–331.

Hoang, D.T., Chernomor, O., von Haeseler, A., Minh, B.Q. & Le, S.V. (2017) UFBoot2: Improving the Ultrafast Bootstrap Approximation. *Molecular Biology and Evolution*, 35, 518–522.
https://doi.org/10.1093/molbev/msx281

Houttuyn, M. (1782) Het onderscheid der salamanderen van de haagdissen in ‘t algemeen, en van de gekkos in ‘t byzonder aangetoond. Verhandelingen Uitgegeven door het *Zeeuwsch Genootschap der Wetenschappen te Vlissingen*, Series 1, 9, 305–336.

Huelsenbeck, J.P., Ronquist, F., Nielsen, R. & Bollback, J.P. (2001) Bayesian Inference of phylogeny and its impact on evolutionary biology. *Science*, 294, 2310–2314. https://doi.org:10.1126/science.1065889

Jackson, D.A. (1993) Stopping rules in principle component analysis: a comparison of heuristical and statistical approaches. *Ecology*, 74, 2204–2214.
https://doi.org/10.2307/1939574

Jombart, T., Devillard, S. & Balloux, F. (2010) Discriminant analysis of principal components: a new method for the analysis of genetically structured populations. *BMC Genetics*, 11, 94.
https://doi.org/10.1186/1471-2156-11-94

Katoh, M. &Kuma, M. (2002) MAFTT: a novel method for rapid sequence alignment based on fast Fourier transform. *Nucleic Acids Research*, 30, 3059–3066. https://doi.org/10.1093/nar/gkf436

Kluge, A.G. (2001) Gekkonid lizard taxonomy. *Hamadryad*, 26, 1–209.

Knowles, L.L. & Carstens, B.C. (2007) Delimiting species without monophyletic gene trees. *Systematic Biology*, 56, 887–895.
https://doi.org/10.1080/10635150701701091

Kuhl, H. & van Hasselt, J.C. (1822) Aus einem Schreiben von Dr. Kuhl und Dr. van Hasselt auf Java. An Professor Th. van Swideren zu Gröningen. *Isis von Oken, Jena*, 6, 472–476.

Kumar, S., Stecher, G. & Tamura, K. (2016) MEGA7: Molecular evolutionary genetics analysis Version 7.0 for bigger datasets. *Molecular Biology and Evolution*, 33, 1870–1874.
https://doi.org/10.1093/molbev/msw054

Kunya, K., Pauwels, O.S.G., Sairum, P. & Taokratok, A. (2011) Squamata, Gekkonidae, *Ptychozoon trinotaterra* Brown, 1999: rediscovery in Thailand. *Check List*, 7, 820–822.
https://doi.org/10.15560/11043

Leaché, A.D., Koo, M.S., Spencer, C.L., Papenfuss, T.J., Fisher, R.N. & McGuire, J.A. (2009) Quantifying ecological, morphological, and genetic variation to delimit species in the coast horned lizard species complex (*Phrynosoma*). *Proceedings of the National Academy of Sciences*, 106, 12418–12423.
https://doi.org/10.1073/pnas.0906380106

Leong, T.-M., Grismer, L.L. & Mumpuni (2003) Preliminary checklists of the Anambas and Natuna Islands (South China Sea). *Hamadryad*, 27, 65–174.

Lleonart, J., Salat, J. & Torres, G.J. (2000) Removing allometric effects of body size in morphological analysis. *Journal of Theoretical Biology*, 205, 85–93.
https://doi.org/10.1006/jtbi.2000.2043

Macey, J.J., Larson, A., Ananjeva, N.B., Fang, Z. & Papenfuss, T.J. (1997) Two novel gene orders and the role of light-strand replication in rearrangement of the vertebrate mitochondrial genome. *Molecular Biology and Evolution*, 14, 91–104.
https://doi.org/10.1093/oxfordjournals.molbev.a025706

Maddison, W.P. & Maddison, D.R. (2015) *Mesquite: a modular system for evolutionary analysis. Version 3.04*. Available from: http://mesquiteproject.org (accesed 20 May 2019)

Malhotra, A., Thorpe, R.S., Mrinalini & Stuart, B.L. (2011) Two new species of pitviper of the genus *Cryptelytrops* Cope 1860

(Squamata: Viperidae: Crotalinae) from Southeast Asia. *Zootaxa*, 2757 (1), 1–23. https://doi.org/10.11646/zootaxa.2757.1.1

Manthey, U. & Grossmann, W. (1997) *Amphibien & Reptilien Südostasiens*. Natur und Tier Verlag, Münster, 512 pp.

Manthey, U. & Manthey, S. (2017) Amphibien und Reptilian von Laos—ein Reisebericht. Teil 1: Phou Khao Khouay NBCA (Februar 1998). *Sauria*, 39, 35–55.

Marcellini, D.L. & Keefer, T.E. (1976) Analysis of the gliding behavior of *Ptychozoon lion-atum* (Reptilia: Gekkonidae). *Herpetologica*, 32, 362–66.

Miller, M.A., Pfeiffer, W. & Schwartz, T. (2010) Creating the CIPRES Science Gateway for inference of large phylogenetic trees. *In*: *Proceedings of the Gateway Computing Environments Workshop (GCE), New Orleans, LA*, 14 November 2010, pp. 1–8. https://doi.org/10.1109/GCE.2010.5676129

Murdoch, M.L., Grismer, L.L., Wood Jr., P.L., Neang, T., Poyarkov, N.A., Ngo, V.T., Nazarov, R., Aowphol, A., Pauwels, O.S.G., Nguyen, H.N. & Grismer, J.L. (2019) Six new species of the *Cyrtodactylus intermedius* complex (Squamata: Gekkonidae) *intermedius* complex from the Cardamom Mountains and associated highlands of Southeast Asia. *Zootaxa*, 4554 (1), 1–62. https://doi.org/10.11646/zootaxa.4554.1.1

Nguyen, L.-T., Schmidt, H.A., von Haeseler, A. & Minh, B.Q. (2015) IQ-TREE: A fast and effective stochastic algorithm for estimating maximum likelihood phylogenies. *Molecular Biology and Evolution*, 32, 268–274. https://doi.org/10.1093/molbev/msu300

Nguyen, V.S., Ho. T.C. & Nguyen, T.Q. (2009) *Herpetofauna of Vietnam.* Edition Chimaira, Frankfurt am Main, 768 pp.

Oksanen, J.G., Blanchet, F.G., Friendly, M., Kindt, R., Legendre, P., McGlinn, D., Minchin, P.R., O'Hara, R.B., Simpson, G.L., Solymos, P., Henry, M., Stevens, H., Szoecs, E. & Wagner, H. (2018) *Community ecology package*. Available from: https://github.com/vegandevs/vegan (accessed 28 January 2019)

Pauwels, O.S.G., Laohawat, O.-A., David, P., Bour, R., Dangsee, P., Puangjit, C. & Chimsunchart, C. (2000) Herpetological investigations in Phang-Nga Province, southern peninsular Thailand, with a list of reptile species and notes on their biology. *Dumerilia*, 4 (2), 123–154.

Pauwels, O.S.G., Laohawat, O.-A., Naaktae, W., Puangjit, C., Wisutharom, T., Chimsunchart, C. & David, P. (2002) Reptile and amphibian diversity in Phang-nga Province, southern Thailand. *Natural History Journal of Chulalongkorn University*, 2 (1), 25–30.

Pawar, S. & Biswas, S. (2001) First record of the Smooth-backed Parachute Gecko *Ptychozoon lionotum* Annandale 1905 from the Indian mainland. *Asiatic Herpetological Research*, 9, 101–106.

Pons, J., Barraclough, T.G., Gomez-Zurita, J., Cardoso, A., Duran, D.P, Hazell, S., Kamoun, S., Sumlin, W.D. & Vogler, A.P. (2006) Sequence-based species delimitation for the DNA taxonomy of undescribed insects. *Systematic Biology*, 55, 595–609. https://doi.org/10.1080/10635150600852011

Quah, E.S.H & Anuar, S. (2018) Amphibians and reptiles of the Malaysian-Thai border regions. *Journal of Wildlife and Parks*, 33, 15–29.

R Core Team (2015) *R: A language and environment for statistical computing*. R Foundation for Statistical Computing, Vienna. Available from: http://www.R-project.org (accessed 29 December 2016)

Rambaut, A. & Drummond, A.J. (2013) *TreeAnnotator. Version 1.8.0. MCMC Output Analysis*. Available from: http://beast.community/treeannotator (accessed 20 May 2019)

Rambaut, A., Suchard, M.A., Xie, D. & Drummond, A.J. (2014) *Tracer. Vol. 1.6*. Available from http//dx.doi.org:beast.bio.ed.ac.uk/Tracer (accessed 20 May 2019)

Ripley, B., Venables, B., Bates, D.M., Hornik, K., Gebhardt, A. & Firth, D. (2018) *Support functions and databases for Venables and Ripley's MASS*. Available from: http://www.stats.ox.ac.uk/pub/MASS4/ (accessed 20 May 2019)

Ronquist, F., Teslenko, M., van der Mark, P., Ayres, D.L., Darling, A., Höhna, B., Larget, L., Liu, L., Suchard, M.A. & Huelsenbeck, J.P. (2012) Mr. Bayes 3.2: efficient Bayesian phylogenetic inference and model choice across a large model space. *Systematic Biology*, 61, 539–542. https://doi.org/10.1093/sysbio/sys029

Russell, A.P., Dijkstra, L.D. & Powell, G.L. (2001) Structural characteristics of the patagium of *Ptychozoon kuhli* (Reptilia: Gekkonidae) in relation to parachuting locomotion. *Journal of Morphology*, 247, 252–263. https://doi.org/10.1002/1097-4687(200103)247:3<252::aid-jmor1015>3.3.co;2-q

Sabaj, M.H. (2016) *Standard symbolic codes for institutional resource collections in herpetology and ichthyology: an Online Reference. Version 6.5 (16 August 2016)*. American Society of Ichthyologists and Herpetologists, Washington, D.C. Electronically accessible. Available from: http://www.asih.org/ (accessed 20 May 2019)

Shaw, K.L. (2002) Conflict between nuclear and mitochondrial DNA phylogenies of a recent species radiation: what mtDNA reveals and conceals about modes of speciation in Hawaiian crickets. *Proceedings of the National Academy of Sciences of the United States*, 99, 16122–16127. https://doi.org/10.1073/pnas.242585899

Sheridan, J.A. & Stuart, B.L. (2018) Hidden species diversity in *Sylvirana nigrovittata* (Amphibia: Ranidae) highlight the importance of taxonomic revisions in biodiversity conservation. *PLoS ONE*, 13, e0192766. https://doi.org/10.1371/journal.pone.0192766

Smith, M.A. (1935) *Fauna of British India, including Ceylon and Burma. Reptilia and Amphibia*. *Vol. II. Sauria*. Taylor &

Francis Ltd., London, 440 pp.
Stejneger, L. (1902) *Ptychozoon kuhli*, a new name for *P. homalocephalum*. *Proceedings of the Biological Society of Washington*, 15, 37.
Stejneger, L. (1907) A new geckoid lizard from the Philippine Islands. *Proceedings of the United States National Museum*, 33, 545–546.
https://doi.org/10.5479/si.00963801.1576.545
Stuart, B.L. & Emmett, D.A. (2006) A collection of amphibians and reptiles from the Elephant and Cardamom Mountains, southwestern Cambodia. *Fieldiana Zoology*, New Series, 109, 1–27.
https://doi.org/10.3158/0015-0754(2006)109[1:acoaar]2.0.co;2
Stuart, B.L., Inger, R.F. & Voris, H.K. (2006) High level of cryptic species diversity revealed by sympatric lineages of Southeast Asian forest frogs. *Biology Letters*, 2, 470–474.
https://doi.org/10.1098/rsbl.2006.0505
Sukumaran, J. & Knowles, L.L. (2017) Multispecies coalescent delimits structure, not species. *Proceedings of the National Academy of Sciences*, 114, 1607–1612.
https://doi.org/10.1073/pnas.1607921114
Sumontha, M., Pauwels, O.S.G., Kunya, K., Limlikhitaksorn, C., Ruksue, S., Taokratok, A., Ansermet, M. & Chanhome, L. (2012) A new species of Parachute Gecko (Squamata: Gekkonidae: genus *Ptychozoon*) from Kaeng Krachan National Park, western Thailand. *Zootaxa*, 3513 (1), 68–78.
https://doi.org/10.11646/zootaxa.3513.1.4
Taylor, E.H. (1915) New species of Philippine lizards. *Philippine Journal of Science*, 10, 89–109.
Taylor, E.H. (1922) Additions to the herpetological fauna of the Philippine Islands, I. *Philippine Journal of Science*, 21, 161–206.
https://doi.org/10.5962/bhl.part.25389
Taylor, E.H. (1963) The lizard fauna of Thailand. *The University of Kansas Science Bulletin*, 54, 687–1077.
Teynié, A., Nguyen, T.Q., Lorvelec, O., Piquet, A., Lottier, A. & David, P. (2014) Amphibiens et reptiles du Laos: nouvelles données nationales et provincials. *Bulletin de la Société Herpétologique de France*, 151, 21–52.
Thorpe, R.S. (1975) Quantitative handling of characters useful in snake systematics with particular reference to interspecific variation in the Ringed Snake *Natrix natrix* (L.). *Biological Journal of the Linnean Society*, 7, 27–43.
https://doi.org/10.1111/j.1095-8312.1975.tb00732.x
Thorpe, R.S. (1983) A review of the numerical methods for recognizing and analysing racial differentiation. *In*: Felsenstein, J. (Ed.), *Numerical Taxonomy. NATO ASI Series (Series G: Ecological Sciences). Vol. 1*. Springer-Verlag, Berlin, pp. 404–423.
https://doi.org/10.1007/978-3-642-69024-2_43
Toews, D.P.L.J. & Brelsford, A. (2012) The biogeography of nuclear discordance in animals. *Molecular Ecology*, 21, 3907–3930.
https://doi.org/10.1111/j.1365-294x.2012.05664.x
Turan, C. (1999) A note on the examination of morphometric differentiation among fish populations: the truss system. *Turkish Journal of Zoology*, 23, 259–263.
Uetz, P., Freed, P. & Hošek, J. (Eds.) (2019) *The Reptile Database*. Available from: http://www.reptile-database.org/ (accessed 19 January 2019)
Vassilieva, A.B., Galoyan, E.A, Poyarkov, N.A. & Geissler, P. (2016) *A photographic Field Guide to the Amphibians and Reptiles of the Lowland Monsoon Forests of Southern Vietnam.* Edition Chimaira, Frankfurt am Main, 324 pp.
Wang, Y.-Y., Wang, J. & Liu, Z.-Y. (2016) Description of a new species of the genus *Ptychozoon* (Squamata: Gekkonidae), representing a new national record of this genus from southern Yunnan Province, China. *Zootaxa*, 4084 (3), 406–420.
https://doi.org/10.11646/zootaxa.4084.3.6
Wilcox, T.P., Zwickl, D.J., Heath, T.A. & Hillis, D.M. (2002) Phylogenetic relationships of the dwarf boas and a comparison of Bayesian and bootstrap measures of phylogenetic support. *Molecular Phylogenetics and Evolution*, 25, 361–371. https://doi.org/10.1016/S1055-7903(02)00244-0
Young, B.A., Lee, C.E. & Daley, K.M. (2002) On a flap and a foot; aerial locomotion in the "flying" gecko, *Ptychozoon kuhli*. *Journal of Herpetology*, 36, 412–418.
https://doi.org/10.1670/0022-1511(2002)036[0412:OAFAAF]2.0.CO;2